



Open Archive Toulouse Archive Ouverte


OATAO is an open access repository that collects the work of Toulouse researchers and makes it freely available over the web where possible

This is an author's version published in: <http://oatao.univ-toulouse.fr/21291>

Official URL:

<https://doi.org/10.1016/j.ecolmodel.2018.10.018>

To cite this version:

Laplanche, Christophe  and Leunda, Pedro M. and Boithias, Laurie and Ardaíz, José and Juanes, Francis *Advantages and insights from a hierarchical Bayesian growth and dynamics model based on salmonid electrofishing removal data.* (2019) Ecological Modelling, 392. 8-21. ISSN 0304-3800

Any correspondence concerning this service should be sent to the repository administrator: tech-oatao@listes-diff.inp-toulouse.fr

Advantages and insights from a hierarchical Bayesian growth and dynamics model based on salmonid electrofishing removal data

Christophe Laplanche^a, Pedro M. Leunda^b, Laurie Boithias^c, José Ardaíz^d, Francis Juanes^e

^a*EcoLab, Université de Toulouse, CNRS, INPT, UPS, Toulouse, France*

^b*Gestión Ambiental de Navarra S.A., c/ Padre Adoain 219 Bajo, 31013 Pamplona/Iruña, Navarra, Spain*

^c*GET, Université de Toulouse, CNRS, IRD, UPS, Toulouse, France*

^d*Gobierno de Navarra, Departamento de Desarrollo Rural y Medio Ambiente, c/ Gonzalez Tablas 9, 31005 Pamplona/Iruña, Navarra, Spain*

^e*Department of Biology, University of Victoria, Victoria, BC, V8W 3N5, Canada*

Abstract

Growth is a fundamental ecological process of stream-dwelling salmonids which is strongly interrelated to critical life history events (emergence, mortality, sexual maturity, smolting, spawning). The ability to accurately model growth becomes critical when making population predictions over large temporal (multi-decadal) and spatial (meso) scales, e.g., investigating the effect of global change. Body length collection by removal sampling is a widely-used practice for monitoring fish populations over such large scales. Such data can be efficiently integrated into a Hierarchical Bayesian Model (HBM) and lead to interesting findings on fish dynamics. We illustrate this approach by presenting an integrated HBM of brown trout (*Salmo trutta*) growth, population dynamics, and removal sampling data collection processes using large temporal and spatial scales data (20 years; 48 sites placed along a 100 km latitudinal gradient). Growth and population dynamics are modelled by ordinary differential equations with parameters bound together in a hierarchical structure. The observation process is modelled with a combination of a Poisson error, a binomial error, and a mixture of Gaussian distributions. Absolute fit is measured using posterior predictive checks, which results indicate that our model fits the data well. Results indicate that growth rate is positively correlated to catchment area. This result corroborates those of other studies (laboratory, exploratory) that identified factors besides water temperature that are related to daily ration and have a significant effect on stream-dwelling salmonid growth at a large scale. Our study also illustrates the value of integrated HBM and

electrofishing removal sampling data to study *in situ* fish populations over large scales.

Keywords: **Growth, Population dynamics, *Salmo trutta*, Depletion sampling, Iberian peninsula, Mesoscale**

1. Introduction

Growth is a fundamental ecological process of most organisms. This is especially true for fishes for three reasons. First, fish continue to grow through their lifetime, i.e. they have indeterminate growth, and body size can increase by several orders of magnitude (from an average size of 1 mm at the egg stage to several meters in the largest species) (Summerfeldt & Hall, 1987; Jobling, 2002). Second, growth rate is dynamic through the life history, typically high in early life and slower later in life, is the most variable component of fish energy budgets (Jobling, 2002), and can respond quickly in a compensatory fashion to changed conditions (Ali et al., 2003). Third, fish growth is driven by a variety of factors including genetics and both abiotic and biotic factors, as demonstrated both in the lab (Brett et al., 1969; Elliott, 1975a,b; Coleman & Fausch, 2007b) and *in situ* (Coleman & Fausch, 2007a; Robinson et al., 2010; Xu et al., 2010; Letcher et al., 2015). Because most fish are ectothermic, their growth is especially sensitive to environmental variation, particularly temperature. But growth also responds in a context-specific way to interactions among multiple abiotic and biotic factors (Klemetsen et al., 2003) and as such is tightly related to population dynamics. In stream-dwelling salmonids, growth is sensitive to a wide variety of factors, including temperature, discharge, elevation, and conspecific density (Table 1, for a range of species) and is also strongly correlated with critical life history events (Hutchings, 2002; Pepin, 2016). For example, growth can determine smolting age, size and age at migration, overwinter mortality, return timing, sexual maturity, success on the spawning grounds and emergence time of embryos, among others (Quinn, 2005; Levings, 2016). However, disentangling the relative importance of biotic and abiotic factors remains challenging as each is dynamic and either tightly related to climate and hydrology or to population dynamics, all of which have been shown to be sensitive to global climate change. The ability to accurately model fish growth and population dynamics thus becomes critical when making predictions about the future, e.g. effects of changes in both land use and climate (Parra et al., 2009, 2012; Boithias et al.,

28 2014) on salmonid population dynamics (Milner et al., 2003; Jonsson & Jonsson, 2009;
29 Baumann et al., 2012; Martins et al., 2012; Kovach et al., 2016; Clavero et al., 2017).

30 Two main approaches are made available for researchers and managers to monitor
31 growth and dynamics of salmonid populations in the field: Individual Tagging Methods
32 (ITM, e.g., using Passive Integrated Transponder ‘PIT’ tags) and Removal Sampling by
33 ElectroFishing (EFRS). ITM provides information about individuals but are expensive
34 to operate at a large spatial scale (although this is possible; Marvin (2012)). EFRS is
35 less precise about some aspects, by providing information on open groups of individuals,
36 but requires less sampling time (see below). In view of their relative advantages, ITM
37 and EFRS have both been used to monitor growth and dynamics of freshwater salmonid
38 populations in the field, although EFRS is more common when studying growth (Table
39 1).

40 Two main reasons explain the popularity of EFRS: the relatively short sampling time
41 it requires to collect data and the ease and wide variety of methods that can be used
42 with it to compute maximum likelihood estimates of population size (reviewed by Cowx
43 (1983)). Another option is to use a dedicated software for a wider choice of models (e.g.,
44 MARK, although its main use is for ITM data, White & Burnham (1999)). The ease of
45 monitoring fish populations with EFRS has led to uninterrupted series of long-term data
46 over large spatial scales, usually collected for management perspectives and later used for
47 research (see for instance Parra et al. (2009); Filipe et al. (2013); Bergerot et al. (2015)).

48 Monitoring fish populations with EFRS (e.g., to estimate recruitment or mortality
49 rates) includes measuring fish age. Calcified structures –otoliths or scales– can be sampled
50 (lethally or non-lethally, respectively) on collected individuals and used to estimate fish
51 age (Dortel et al., 2013). An alternative to otoliths and scales for fishes in temperate
52 climates is to measure the length of collected individuals and infer population structure
53 from the statistical distribution of length data. This is possible for stream-dwelling trout
54 because the length distribution is multimodal, with one component per year of emergence
55 (‘cohort’). The main reason for the multimodality is that reproduction occurs during
56 a short period in autumn/winter (Isely & Grabowski, 2007). Many statistical methods
57 are available to managers to easily separate overlapping length distributions across ages
58 (Pitcher, 2002). Individual fish length is consequently collected during EFRS surveys

59 (later referred to as ‘EFRS length data’), thus providing long-term data over large spatial
60 scales, ideal for investigating effects of global change on the growth and dynamics of
61 salmonid populations (Naslund et al., 1998; Parra et al., 2009; Filipe et al., 2013; Bergerot
62 et al., 2015; Kanno et al., 2015).

63 More recently, Hierarchical Bayesian Modelling (HBM) has increased the interest in
64 using EFRS data to study stream-dwelling salmonid ecology (also applies to ITM data,
65 see Kéry & Schaub (2012)). One main reason for the renewed interest is that the HBM
66 framework offers the ability to build observation models that are connected to ecological
67 models, both possibly advanced (e.g., more than what dedicated tools such as MARK
68 can offer), as integrated models (Letcher et al., 2015). More specifically, HBMs have
69 proven to effectively model EFRS observations (Rivot et al., 2008), multimodal length
70 distributions (Ruiz & Laplanche, 2010), growth (He & Bence, 2007; Bal et al., 2011;
71 Lecomte & Laplanche, 2012; Sigourney et al., 2012; Dortel et al., 2013), and population
72 dynamics (Kanno et al., 2015; Bret et al., 2017). Other reasons for the growing popularity
73 of HBMs include their ability to propagate uncertainty from observations to parameter
74 estimates and to compare competing models to test hypotheses (Lunn et al., 2013). The
75 HBM framework also allows the use of prior distribution with model parameters (e.g.,
76 based on earlier studies) and definition of a hierarchical structure that facilitates spatial
77 inter-/extrapolation and forecasting (Banerjee et al., 2004; Lunn et al., 2013).

78 While raw EFRS length data have been used to infer somatic growth (Lecomte &
79 Laplanche, 2012), and pre-processed length data (into mean-length-at-age and density-at-
80 age estimates) have been used to model either growth or population dynamics separately
81 (e.g., He et al. (2008); Laplanche et al. (2018)), to our knowledge, raw EFRS length
82 data have never been used to infer growth and population dynamics at the same time
83 as an integrated model. We thus present an integrated HBM that models observations,
84 somatic growth, and basic population dynamics. We illustrate the capabilities of the
85 modelling framework by applying it to long-term data collected over a large spatial scale
86 (*Salmo trutta*; 20 years; 48 sites). There is an apparent wide diversity of factors that
87 affect stream-dwelling salmonid growth *in situ* (Table 1), which results of our modelling
88 approach help explain. We further highlight advantages of our integrated approach and
89 suggestions for potentially rewarding model extensions.

90 2. Materials and methods

91 2.1. Growth, population dynamics, and observation models

92 As mentioned, reproduction of stream-dwelling salmonids follows a yearly pattern.
93 In contrast, growth is continuous. We thus needed to define two time structures: an
94 index over years-of-emergence i.e. cohorts ($y \in \{1, \dots, Y\}$; $y = 1$ for the first modelled
95 cohort; Y consecutive cohorts) and an additional continuous time variable (t , in days;
96 $t = 0$ on January 1st of year $y = 1$). To simplify presentation, equations are presented
97 below as if there were only one sampled/modelled location. The spatial dimension and
98 the hierarchical structure of the model are presented later (section 2.2).

99 2.1.1. Modelling the time/size at emergence

100 Times of emergence are strongly year-dependent, because spawning is mainly triggered
101 by a decline in photoperiod and temperature (Jonsson & Jonsson, 2009), and because
102 development of trout eggs from spawning to emergence is mainly driven by water tem-
103 perature (Elliott & Hurley, 1998; Ojanguren & Braña, 2003; Jonsson & Jonsson, 2009).
104 Additional inter-individual differences in spawning times (spawning lasts for several weeks
105 around a peak of activity; e.g., Riedl & Peter (2013); Isely & Grabowski (2007)) are
106 magnified by inter-individual differences in the development of eggs and parr, causing
107 inter-individual differences in emergence times for a given year. We define d_y^{emerg} (day)
108 as the (year-dependent) median time of emergence, i.e. the day of year y when half the
109 fry have emerged.

110 Many studies identified additional inter-individual variation in size at emergence. As it
111 was not possible to disentangle variation in both time and size at emergence with EFRS
112 length data alone, we model inter-individual variation in both the time of and size at
113 emergence as a single source of variation, in the form of the distribution of theoretical fish
114 length at time d_y^{emerg} . While we consider d_y^{emerg} an unknown parameter in the model, we
115 assume that mean trout length at emergence is known and constant. We denote L^{emerg}
116 (in mm) this quantity, i.e. mean length at time d_y^{emerg} of the cohort which emerged in
117 year y .

118 *2.1.2. Modelling cohort growth*

119 The growth model which follows is the consequence of a similar model working at the
 120 individual fish level with random variation of growth parameters among individuals. We
 121 present the individual growth model in Appendix A and keep to the cohort level in the
 122 following, which is of greater interest given the available data (e.g., EFRS length data).
 123 One central assumption of the cohort growth model is that fish of a given cohort grow
 124 under similar environmental conditions. This is the case for stream-dwelling salmonids,
 125 due to limited movement, which includes long-distance return migration for reproduction,
 126 meso-habitat movement as habitat needs change through their life-time, and daily micro-
 127 habitat movements (Schlosser, 1991; Gido & Jackson, 2010; White et al., 2014; Matthews
 128 & Hopkins, 2017; Laplanche et al., 2018).

The mean length at time t of the cohort which emerged on year y is denoted $\mu_y(t)$,
 where t highlights the fact that growth is time-dependent, and subscript y specifies that
 mean length is also year-of-emergence dependent, since several cohorts exist at the same
 time. Cohort growth is modelled as

$$\frac{d\mu_y(t)}{dt} = H_y(t) \quad \text{for } t \geq d_y^{emerg}, \quad (1)$$

129 starting from $\mu_y(d_y^{emerg}) = L^{emerg}$, where $H_y(t)$ is daily length increase, which is also
 130 year-of-emergence dependent and time dependent.

131 Growth rate of stream-dwelling salmonids decreases with fish age, which can be appro-
 132 priately modelled using empirical, concave growth functions (von Bertalanffy, Gompertz,
 133 etc.). We follow Elliott et al. (1995), who modelled growth as linear for certain powers
 134 of weight, and retain some of their notations to further facilitate comparison of results.
 135 Hence, growth rate is expressed as

$$\frac{d(W_y(t)^b)}{dt} = b \frac{G_y(t)}{100} \quad \text{for } t \geq d_y^{emerg}, \quad (2)$$

136 where $W_y(t)$ is the mean weight at time t of the cohort which emerged in year y , b is the
 137 power when weight raised to this power grows linearly, and $G_y(t)$ is a year-of-emergence
 138 dependent and time-dependent parameter. In the case of a one-to-one length-weight
 139 relationship ($W_y(t) = a_w \mu_y(t)^{b_w}$; see data section), the model is equivalent to having
 140 daily length increase proportional to the power of length

$$\frac{d\mu_y(t)}{dt} = \frac{1}{b_w a_w^{1/b_w}} \frac{G_y(t)}{100} \mu_y(t)^{1-bb_w}. \quad (3)$$

141 Growth curves covered by this ‘power growth model’ are illustrated in Appendix S1.
 142 High correlation between growth parameters b and $G_y(t)$, due to multiplying them in eq.
 143 (2), and as illustrated in Appendix S1, compels us to set one of the two parameters as a
 144 constant, in our case b , and be more flexible on the other, $G_y(t)$.

The effect of water temperature on growth rate is introduced into the model by defining

$$G_y(t) = X(T^w(t))G'_y(t), \quad (4)$$

145 where $X(T^w(t))$ models the effect of temperature on growth and $G'_y(t)$ is a random effect
 146 (defined later). The function $X \in [0, 1]$ defines the suitability of water temperature for
 147 growth, equaling to 0 below a minimum (T^{min}) and above a maximum water temperature
 148 (T^{max}), and reaching 1 at an optimal temperature (T^{opt}). We chose a rational function
 149 (e.g., Mallet et al. (1999)).

150 In sum, daily growth rate is the product of 3 terms: $\mu_y(t)^{1-bb_w}/100b_w a_w^{1/b_w}$, which
 151 models a decrease in growth rate with increasing age; $X(T^w(t))$, which models the suit-
 152 ability of water temperature for growth; and $G'_y(t)$, which accounts for other sources of
 153 variation.

154 2.1.3. Modelling growth dispersion

155 Differences in growth trajectories among individual fish led us to model distribution of
 156 trout length at any time of a given cohort with a normal distribution (Appendix A). The
 157 individual growth model also led us to express the standard deviation of length within
 158 a cohort (denoted $\sigma_y(t)$) as proportional to its mean, thus modelling the spread of the
 159 length distribution of cohorts over time, as follows

$$\sigma_y(t) = \nu \mu_y(t), \quad (5)$$

160 where the coefficient of variation (CV) ν is a direct measure of the variation in growth
 161 rates among individual fish (Appendix A).

162 *2.1.4. Modelling the distribution of fish length*

163 Because of the normal distribution of trout length within a cohort, trout length from
 164 all the included cohorts is modelled as a mixture of Gaussian distributions, one component
 165 per age (Figure 1). The theoretical probability density function of trout length at time t
 166 is consequently

$$f(t, x) = \sum_{k=1}^K \frac{\lambda_{y(t)-k+1}(t)}{\lambda(t)} \frac{1}{\sqrt{2\pi}\sigma_{y(t)-k+1}(t)} \exp\left(-\frac{(x - \mu_{y(t)-k+1}(t))^2}{2\sigma_{y(t)-k+1}(t)^2}\right), \quad (6)$$

167 where x is trout length in mm, $y(t)$ is the year which corresponds to time t , $y(t) - k + 1$ is
 168 the year-of-emergence of the cohort that is age k in year $y(t)$, $k \in \{1, \dots, K\}$ is an index
 169 over age ($k = 1$ for trout of age 0, referred to as trout of age 0+; $k = 2$ for trout of age 1,
 170 referred to as trout of age 1+; etc.), K is the maximum age in the model, and $\lambda_y(t)$ (m^{-2})
 171 is the density at time t of the cohort that emerged in year y ; $\lambda(t) = \sum_{k=1}^K \lambda_{y(t)-k+1}(t)$ is
 172 the overall trout density at time t .

173 Fish length range is divided into L intervals of width Δx (mm), from 0 to maximum
 174 length $x_{max} = L\Delta x$ (mm) (class centers are denoted $x_l = (l - 1/2)\Delta x$ in mm; $l \in$
 175 $\{1, \dots, L\}$ is an index over length classes). The expected density of fish of size class l at
 176 time t is therefore $\lambda_l(t) = \lambda(t) \int_{(l-1)\Delta x}^{l\Delta x} f(t, x) dx \text{ m}^{-2}$.

177 *2.1.5. Modelling observations*

The number of fish actually present is modelled as a Poisson variate (Wyatt, 2002)

$$N_l(t) \sim \text{Poisson}(A\lambda_l(t)), \quad (7)$$

178 where A (m^2) is the area which is sampled by EFRS. The Poisson distribution models
 179 stochasticity of fish presence and assumes that the distributions of individuals for a given
 180 size class are independent of one another and are not spatially structured, e.g., via physical
 181 habitat characteristics (Peterson, 1999).

The number of fish of size class l caught at time t by electrofishing the area during
 removal r , observations of which were referred to as EFRS length data, is modelled as a
 binomial variate (Wyatt, 2002; Kanno et al., 2015)

$$C_{l,r}(t) \sim \text{Binomial}(R_{l,r}(t), p_{l,r}(t)), \quad (8)$$

182 where $R_{l,1}(t) = N_l(t)$ and $R_{l,r}(t) = R_{l,r-1}(t) - C_{l,r-1}(t)$ ($r \geq 2$) is the stock left before
 183 removal r . The binomial distribution models stochasticity of fish capture by assuming
 184 that capture of fish of a given size class in the sampled area is independent with the
 185 same probability. Capture probability $p_{l,r}(t)$ increases with increasing fish size, which is
 186 modelled as $\text{logit}(p_{l,r}(t)) = \alpha x_l/1000 + \beta$.

187 2.1.6. Modelling population dynamics

We interrelate densities of cohorts for subsequent years as follows

$$\frac{d\lambda_y(t)}{dt} = (\text{Sur}_y(t) - 1)\lambda_y(t) \quad \text{for } t \geq d_y^{emerg}, \quad (9)$$

188 starting from $\lambda_y(d_y^{emerg}) = \lambda_y^{emerg}$, where λ_y^{emerg} is density at time d_y^{emerg} (recruitment)
 189 and $\text{Sur}_y(t)$ is the apparent survival rate between t and $t + 1$ of the cohort that emerged
 190 in year y . Apparent survival can be < 1 due to prevailing mortality or outgoing net
 191 displacements, or > 1 when mortality is balanced by incoming net displacements from
 192 area A .

193 2.2. The Hierarchical Bayesian Model

194 The growth, population dynamics, and observation models presented in the previous
 195 section were combined into an integrated HBM, as follows. Indices defined earlier are
 196 used in the HBM (year y , age k , removal r , and length class l). Specific details of our case
 197 study, namely the species (brown trout; see section 2.2.1) and the data sampling scheme
 198 (one EFRS survey a year; see section 2.2.2), are reflected in the temporal structure of the
 199 model. Moreover, EFRS surveys were conducted at multiple locations, which results in
 200 defining a new index over sites ($s \in \{1, \dots, S\}$; S sites) and a dedicated spatial structure
 201 (see section 2.2.3).

202 Equations and values of the variables of the HBM are shown in Table 2. Relationships
 203 between HBM variables of the growth and population dynamics models are illustrated
 204 with a Directed Acyclic Graph (DAG, Figure 2). HBM variables, either measured or
 205 unknown, may be scalar, vectors, or multi-dimensional, as indicated by their subscript(s).
 206 As an illustration, (known) times of EFRS surveys are grouped together in the variable
 207 $d_{s,y}$ (days), which has 2 dimensions: site and year.

208 *2.2.1. Details due to the study of Salmo trutta*

209 Based on other studies, we chose $L^{emerg} = 30$ mm for the size of emergence (Nika,
 210 2013). We used parameter values published by Elliott et al. (1995) for T^{min} , T^{max} , and
 211 T^{opt} to calculate the temperature-dependent growth rate (Appendix S1). Brown trout is
 212 an autumn spawner, which makes the length distribution of trout of age 0+ observable
 213 in summer, when our sampling took place.

214 *2.2.2. Details due to the temporal structure of the sampling scheme*

215 The data sampling scheme (uninterrupted series of one EFRS survey in summer each
 216 year, see section 2.4) influenced details of the temporal structure of the HBM. The mean,
 217 standard deviation, and density of each component that defines the multimodal distri-
 218 bution of trout length at survey times (eq. (6)) are denoted $\mu_{s,y,k}$ (mm), $\sigma_{s,y,k}$ (mm),
 219 and $\lambda_{s,y,k}$ (m^{-2}), respectively. These parameters play a special role in the HBM by being
 220 directly connected to the growth model (in the case of $\mu_{s,y,k}$ and $\sigma_{s,y,k}$), to the popula-
 221 tion dynamics model ($\lambda_{s,y,k}$), and to the observation model ($\mu_{s,y,k}$, $\sigma_{s,y,k}$, and $\lambda_{s,y,k}$), as
 222 highlighted in the DAG (Figure 2). The resulting expected number of fish in each size
 223 class present in sampled area $A_{s,y}$ at survey times is denoted $E(N_{s,y,l}) = A_{s,y}\lambda_{s,y}f_{s,y,l}$,
 224 where $f_{s,y,l}$ is found by integrating eq. (6) over size class l , and $\lambda_{s,y} = \sum_k \lambda_{s,y,k}$ denotes
 225 overall trout density. The probability of capturing fish during EFRS surveys is denoted
 226 $p_{s,y,l,r}$. EFRS length data, for each site, year, size class, and removal, are gathered into a
 227 4-dimensional contingency table, denoted $C_{s,y,l,r}$.

228 Our sampling scheme also implies that ‘only’ one observation of the multimodal distri-
 229 bution of trout length is available each year. As a result, we defined the random effect in
 230 eq. (4) in our HBM as site- and year-dependent ($G'_{s,y}$). The population dynamics model
 231 reduces to a Markov process, with site-, year-, and age-dependent apparent survival rates
 232 (denoted $Sur_{s,y,k}$) between subsequent survey times. The abundance of trout of age 0+
 233 at survey times is, using the notation defined earlier, $\lambda_{s,y,1}$.

234 Continuous variable t used in the growth, population dynamics, and observation mod-
 235 els becomes a daily time step in the HBM, indexed with $d \in \{1, \dots, D\}$ spanning the
 236 Y years that are considered in the model. Daily mean water temperatures are denoted
 237 $T_{s,d}^w$ in the HBM and growth parameter $G_y(t)$ becomes $G_{s,y,k,d}$. The ordinary differential

238 equation (3) was thus integrated at a daily time step using Euler’s forward method. In
 239 this case, we approximated predicted mean lengths at survey times as

$$\mu_{s,y,k} = \left((L^{emerg})^{bb_w} + \frac{b}{a_w^b} \frac{\Sigma G_{s,y,k}}{100} \right)^{1/bb_w}, \quad (10)$$

240 where $\Sigma G_{s,y,k}$ is the cumulative sum of $G_{s,y,k,d}$ from emergence to observation.

241 Trout of age 1 and older on the year of the first EFRS survey emerged $K - 1$ years
 242 before this year. As a result, we modelled growth and population dynamics $K - 1$ years
 243 before the year of the first EFRS survey. The lack of need of backcasting/forecasting in
 244 our case study led us to model cohorts from this point to the year of the last EFRS survey.
 245 Index y , defined earlier, thus still represents cohorts in the HBM, while the first EFRS
 246 survey corresponds to $y = K$ and the last one to $y = Y$.

247 2.2.3. Spatial structure of the HBM

248 Some quantities defined during model presentation become spatially dependent, which
 249 we highlighted with variable subscript s (Table 2 and Figure 2). Prospective spatial sim-
 250 ilarities of growth rates ($G'_{s,y}$), recruitment ($\lambda_{s,y,1}$), and apparent survival rates ($\text{Sur}_{s,y,k}$)
 251 are modelled as follows

$$\begin{cases} G'_{s,y} \sim \text{Lognormal}(\log(G'_s), \sigma_{G'_s}^2) \\ \lambda_{s,y,1} \sim \text{Lognormal}(\log(\lambda_1), \sigma_{\lambda_1}^2) \\ \text{Sur}_{s,y,k} \sim \text{Lognormal}(\log(\text{Sur}_k), \sigma_{\text{Sur}_k}^2) \end{cases} . \quad (11)$$

252 We chose log-normal distributions to model multiplicative errors for $G'_{s,y}$ and $\text{Sur}_{s,y,k}$ and
 253 to model variation in animal density (Limpert et al., 2001). Hyperparameters $\log(\lambda_1)$,
 254 $\log(\text{Sur}_k)$, $\log(G'_s)$ and $\sigma_{\lambda_1}^2$, $\sigma_{\text{Sur}_k}^2$, $\sigma_{G'_s}^2$ are regional means and variances of $\log(\lambda_{s,y,1})$,
 255 $\log(\text{Sur}_{s,y,k})$, and $\log(G'_{s,y})$, respectively.

256 2.2.4. Priors

257 All model parameters were provided with vague uniform priors (Table 2), between
 258 0 and 1 for λ_1 , Sur_k , b , and ν_s , and between 0 and 10 for σ_{λ_1} , σ_{Sur_k} , G'_s , and $\sigma_{G'_s}$. We
 259 provided time of emergence (denoted $d_{s,y}^{emerg}$) with a uniform prior of a 6-month amplitude
 260 (± 120 days) around a site-dependent, known value.

261 *2.3. Computations and measure of model fit*

262 *2.3.1. Simulating samples of the posterior distribution of the HBM*

263 Equations provided in the previous section can be combined to express the posterior
264 distribution of model parameters. The HBM is, however, too complex for such a distribu-
265 tion to be analytically tractable. Samples from the posterior distribution can be relatively
266 easily simulated via Markov chain Monte Carlo (MCMC), and we used OpenBUGS for
267 this purpose (Lunn et al., 2013). The code of our HBM and a tutorial are both available
268 as Appendix S2. Data pre-processing and output post-processing were implemented in R
269 (R Core Team, 2014). MCMC convergence was assessed by computing inter-chain vari-
270 ances of simulated latent variable samples across 3 chains; initializations were computed
271 using 5, 50, and 95% prior marginal quantiles. After convergence, 5,000 samples were
272 simulated. Only effective sample sizes (ESS) are reported. Point estimates are posterior
273 means.

274 *2.3.2. Absolute measure of model fit*

275 We assessed model fit by comparing the EFRS data collected in the field to their respec-
276 tive values simulated by the model. Observed catch, all removals pooled together, is de-
277 noted $C_{s,y,l} = \sum_r C_{s,y,l,r}$ (Figure 1; sum of the stacked bins for each size class). The distri-
278 butions of the observed ($C_{s,y,l}$) and the expected modelled ($C_{s,y,l}^{pred} = E(N_{s,y,l}) \sum_r p_{s,y,l,r} (1 -$
279 $p_{s,y,l,r})^{r-1}$) distributions of the catches were compared using standard quantile-quantile
280 (Q-Q) plots. A finer comparison of the distributions with a measure of the level of signif-
281 icance of the potentially under- and over-estimated values (for each site, year, and length
282 class) were obtained in a Bayesian framework by using posterior predictive p-values (Gel-
283 man et al., 2004; Lunn et al., 2013; Chambert et al., 2014). For this purpose, replicated
284 data ($C_{s,y,l}^{rep}$) were simulated by the fitted model, which is relatively easy to perform with
285 BUGS (Ntzoufras (2009); Lunn et al. (2013); Appendix S2). The scope of our model
286 checking is to evaluate the fitness of the survey layer (i.e. Poisson-layer and removal sam-
287 pling) given the estimated length distribution, and consequently given values for model
288 hyperparameters such as growth and survival rates. For that reason, replicated data were
289 simulated using the Poisson and Binomial models (eqs (7)-(8)). The desired p-value, as
290 the probability that the replicated data (of size class l , site s , year y) could be more

291 extreme than the observed data, is

$$p_{s,y,l}^B = \Pr(C_{s,y,l}^{rep} \geq C_{s,y,l}). \quad (12)$$

292 P-values lower than 0.05 highlight underestimated values and values greater than 0.95
293 highlight overestimates. P-values of the posterior predictive checks are uniformly dis-
294 tributed if the model fits correctly (Marshall & Spiegelhalter, 2003). We thus compared
295 with another series of Q-Q plots the distributions of the p-values for each site to their theo-
296 retical uniform (0,1) distribution. Computation of the posterior predictive p-values is also
297 relatively easy to perform with BUGS (Ntzoufras (2009); Lunn et al. (2013); Appendix
298 S2).

299 2.4. Study area and data sets

300 2.4.1. Study area

301 The study area represents the natural range of brown trout (*Salmo trutta*) distribution
302 in the region of Navarra (northern Spain, 0°43'–2°29' W, 41°54'–43°19' N). This area of
303 nearly 6,420 km² is geologically heterogeneous (<http://geologia.navarra.es>) and drains
304 northwards into the Bay of Biscay and southwards to the Mediterranean sea via the Ebro
305 river. The Mediterranean drainage of the study area can be further split into two sub-
306 basins that show a clear east-west altitudinal gradient (Figure 3). Elevation in the study
307 area ranges from 0 to 2,444 m.a.s.l.

308 Brown trout is the dominant fish species throughout the study area, and its popula-
309 tions consists exclusively of resident individuals (except for lower reaches of the Atlantic
310 Bidasoa basin, where anadromous individuals exist at low densities). Rivers are open
311 to recreational angling except from some reaches that have preserved sections. Stocking
312 in upper and middle reaches of the study area stopped in 1992 but continues in lower
313 reaches, where brown trout is not the dominant species. Human population density is low
314 in the study area (<10 inhabitants/km²), and rivers are not degraded by anthropogenic
315 land uses or pollution so their ecological status is good or very good (see internal re-
316 ports commissioned by the Department of the Environment of the regional Government
317 of Navarra (DEGN) considering physical-chemical water parameters and biological wa-

318 ter quality). Agricultural land use, hydroelectric power stations, and dams are the main
319 human pressures in the study area (Parra et al., 2009).

320 *2.4.2. EFRS survey network*

321 Electrofishing data were collected by the Fish and Game section of the DEGN (<http://cazaypesca.navarra.es>)
322 The survey network is composed of 61 sampling sites (Figure 3) which are located in every
323 river in upper, middle, and lower reaches and some scattered tributaries. Streams were
324 surveyed once a year every summer (July–September) in 1992-2014 with the exception of
325 5 sites, where sampling started later (2 in 1997; 1999; 2000; 2005). Surveys suspected of
326 being influenced by the presence of stocked individuals were excluded: (1) surveys before
327 1995 and (2) sites in lower reaches where stocking continues (Figure 3). As a result, the
328 survey network we used is composed of 48 sites sampled for 19.5 ± 1.7 consecutive years for
329 a total of $48 \times 20 - 23 = 937$ EFRS surveys. Catchment areas of upstream sampling sites
330 ranged from 9.2 to 614.5 km² (mean: 87.9 km²), and slopes at sampling sites ranged from
331 0.27 to 7.68% (mean: 1.47%). Sampled area differed among sites and years depending on
332 stream width (8.2 ± 3.6 m) and reach length (105.1 ± 35.3 m). The sampling time required
333 to survey 1000 m² ranged from 23 to 127 minutes (mean: 55); variability depending on
334 habitat heterogeneity and fish density.

335 *2.4.3. Fish assessment*

336 One- to three-pass depletion electrofishing was performed, with the two-pass design
337 being the most frequent (not sampled due to surveys started later than 1995: 2.4%; 1
338 removal: 7.0%; 2: 89.2%; 3: 1.5%). Each captured individual was measured for fork
339 length (± 1 mm) before being released, for a total of 189,533 fish-length data samples.
340 Modelling drove us to code fish length data by 10-mm length class. Trout are relatively
341 small in the study area with a short life-span, and thus the maximum size class was set
342 to 400 mm (99% quantile of trout size is 298 mm, length of 146 individuals > 400 mm
343 were truncated to 400 mm) with a maximum age of 4 ($K = 4$). Raw length data collected
344 during EFRS surveys were therefore turned into a 4-dimensional table with the number of
345 trout caught at each site, year, length class, and removal (later referred to as EFRS length
346 data), with missing values depending on when surveys started and how many fish were
347 removed. A total of 14,296 brown trout collected in the study area were also measured

348 for weight. Predicted weights (g) were modelled as $W = a_w L^{b_w}$, where L is length (mm),
349 and $a_w = 1.09 \cdot 10^{-5}$ and $b_w = 3.010$ are the scaling coefficient and exponent respectively
350 ($R^2 > 0.99$; linear regression on log-transformed variables). This relationship was used to
351 convert between length and weight in the growth model (e.g., eq. (10)).

352 *2.4.4. Water temperature*

353 As presented below and in additional detail in Appendix S3, we used air temperature
354 as a proxy for water temperature to calculate values of water temperature at EFRS sites
355 for the entire period (as the model requires). Air temperature, water temperature, and
356 EFRS length data were collected using three independent survey networks, at distinct sites
357 and for different time periods (Figure 3). In short, daily air temperature was spatially
358 interpolated by universal kriging using elevation as a linear predictor with day-dependent
359 regression coefficients. Monthly water temperature was linearly related to monthly air
360 temperature using site-dependent regression coefficients. The seasonal trend in water
361 temperature at EFRS sites was obtained by using the air-water temperature relationship
362 of the nearest water temperature gauge with the seasonal trend in daily air temperatures
363 at EFRS sites as inputs. Simulated water temperatures (range 0.7-23.2°C) covered the
364 range of temperature for brown trout growth (Appendix S1).

365 **3. Results**

366 *3.1. Fish length distribution*

367 The multimodal fish length distribution was predicted for each of the 937 EFRS surveys
368 (Figure 1). QQ-plots of observed vs. expected modelled fish length distributions indicate
369 that the observed and expected modelled distributions of the catch are fairly similar
370 (Figure 4). The results of the posterior predictive checks highlight size classes of under-
371 and over-estimated catch (Figure 1). The combined results of the posterior predictive
372 checks indicate that the model fits correctly, to the exception of site 1620, due to some
373 over-estimated values, and to the exception of sites 1010 and 1830, due to scarce data
374 (Figure 5). From these results, we conclude that the model provides a picture of the
375 distribution of fish length data that is well supported by the data, both in terms of
376 expected values (mixture of multimodal distribution) and dispersion around these values

377 (Poisson and binomial model), thus allowing us to produce and interpret estimates for
378 model's hyperparameters, e.g. related to growth and population dynamics.

379 *3.2. Growth and population dynamics*

380 The model simulates seasonal and interannual growth variation (Figure 6) as well as
381 differences in growth profiles between sites (see below). The estimated value for parameter
382 $b = 0.525$ indicates that growth curves are moderately concave in the study area. Esti-
383 mated values for the growth dispersal parameter (ν_s) ranging from 0.09 to 0.17 (Appendix
384 S4) indicate that growth dispersion is strongly site-dependent.

385 The model also simulates decrease in the apparent survival rate with increasing age
386 (Figure 6), as indicated by estimated values of apparent survival rates at the regional
387 scale (trout of age $0+ \rightarrow 1+$: $\text{Sur}_2 = 0.69$; $1+ \rightarrow 2+$: $\text{Sur}_3 = 0.46$; $2+ \rightarrow 3+$: $\text{Sur}_4 =$
388 0.21). Although not formally tested, respective variances appear similar across age classes
389 ($\sigma_{\text{Sur},2} = 0.76$; $\sigma_{\text{Sur},3} = 0.65$; $\sigma_{\text{Sur},4} = 0.72$). Density of trout of age $0+$ varies greatly
390 among sites, cohorts, and years ($\lambda_1 = 0.077$; $\sigma_{\lambda_1} = 1.40$).

391 Marginal posterior distributions for model parameters (λ_1 , σ_{λ_1} , Sur_k , and $\sigma_{\text{Sur},k}$) are
392 illustrated in Appendix S4.

393 *3.3. Hierarchical structure of growth rate*

394 Daily growth rate was modelled as the product of three terms: size-dependence,
395 temperature-dependence, and other sources of variation. We investigated further the rel-
396 ative contribution of the two latter terms to variation in the daily growth rate. For that
397 purpose, we calculated the variance of the log of the product $X_{s,d}G'_{s,y}$ (0.36), which sums
398 up into the variances of $\log(X_{s,d})$ (0.24) and of $\log(G'_{s,y})$ (0.14) plus twice their covari-
399 ance (-0.05). These results indicate that (1) the deterministic, temperature-dependent
400 term $X_{s,d}$ and the random term $G'_{s,y}$ are weakly correlated with each other (Pearson's
401 $r = -0.13$) and that (2) they contribute respectively and approximately 2/3 and 1/3 of
402 the variance in daily growth rate, size-dependence excluded, on a log-scale.

403 We investigated further the relative contribution of the two latter terms to the mod-
404 elled spatio-temporal variation in daily growth rate. We thus calculated ANOVA sums of
405 squares (SSQ) of both $\log(X_{s,d})$ (using site, year, and month as factors) and $\log(G'_{s,y})$ (us-
406 ing site and year). Percentages of SSQs for each term are shown in Table 3. Results show

407 that one major source of variation in the deterministic, temperature-dependent term is
408 seasonal (month: 30.6%). Two other main contributions highlight the importance of the
409 site-specificity of temporal variation driven by temperature (site*month: 24.7%; site*day:
410 31.7%). Variation in the random term is mainly spatial (site : 73.0%). This analysis also
411 indicates that there is a negligible global trend in the growth rate over the last 20 years
412 (year: 1.5-2.5%), although there is a considerable site-dependent, yearly trend for $G'_{s,y}$
413 (site*year: 24.5%). We did not detect any systematic increase in water temperature over
414 time from 1995-2014, either at each site or at the regional scale (linear regression using
415 mean water temperature).

416 We investigated further reasons for the spatial trend in the random term. We found
417 that G'_s (mean value of $G'_{s,y}$ at each site) increases in streams in the downstream direction
418 (Figure 7). We found that G'_s was weakly correlated with mean water temperature (T_s^w ;
419 log-transformed; $r = -0.13$), indicating that the variation of G'_s in the downstream
420 direction is not due to water warming while flowing downstream. We instead found
421 that G'_s was positively correlated with catchment area (denoted wsa_s ; log-transformed;
422 Pearson's $r = 0.73$) leading towards other possible explanations for spatial variation in
423 growth rate, as discussed later. Parameter G'_s was also negatively correlated with stream
424 slope ($slope_s$; log-transformed; $r = -0.59$). Further linear regression analysis showed that
425 a combination of catchment area and stream slope predicts the random term well, leading
426 to the relationship $\log_{10}(G'_s) = 0.175 \log_{10}(wsa_s/slope_s)$, which explained up to 64% of its
427 variability ($R^2 = 0.64$).

428 4. Discussion

429 4.1. Strength of the approach

430 Collecting fish length data by electrofishing has been used widely for several decades
431 to monitor riverine fish populations. This practice has resulted in long-term monitoring
432 over large spatial scales. Researchers have taken advantage of it to measure, e.g., effects
433 of global change on fish populations (Naslund et al., 1998; Parra et al., 2009; Filipe et al.,
434 2013; Bergerot et al., 2015). The HBM framework has increased the value of EFRS data
435 by allowing the investigation of more challenging scientific questions and the refinement

436 of data use (e.g., large scale data analysis by Kanno et al. (2015)). Our study illus-
437 trates the ability of the HBM framework to consider a relatively complex model for EFRS
438 length observations (mixture of distributions, capture probability increasing with increas-
439 ing fish size, and Poisson/binomial errors), a growth model with a relatively complex
440 hierarchical structure, and a population dynamics model (relatively simple in our case, as
441 a Markov process with a simple hierarchical structure). There are three major advantages
442 in connecting these three models together, or more generally in connecting observation
443 and ecological models together, as an integrated model. The first is to combine diverse
444 datasets by connecting two observation models together (Myers, 2001; Kéry & Schaub,
445 2012). The second is to share parameters both ways by connecting two ecological mod-
446 els together, in our case to model density-dependent somatic growth or size-dependent
447 mortality, which both turned out to be important processes to consider (Sogard, 1997;
448 Imre et al., 2005; Myrvold & Kennedy, 2015). The third is to infer ecological processes
449 from the data, as a result of model calibration, by connecting an ecological model to an
450 observation model (e.g., Laplanche et al. (2018)). Another major advantage in connect-
451 ing an ecological model to an observation model is to ‘enlighten’ data processing with
452 the knowledge brought by the ecological model, in a theory-guided data science paradigm
453 (Karpatne et al., 2017). In our case, consideration of the observation and ecological mod-
454 els as an integrated model allowed us to separate age classes from length frequency data
455 as a function of the ecological processes (growth, mortality). Although the length distri-
456 bution of trout of age 0+ usually clearly stand out from the rest (Crozier et al., 2010;
457 Xu et al., 2010; Logez & Pont, 2011), the distributions of older fish usually overlap due
458 to growth dispersion and growth rate decreasing with fish age, making ‘blind’ separa-
459 tion more challenging, possibly leading to misclassification (Pitcher, 2002; FAO Fisheries
460 and Aquaculture Department, 2013). The subsequent loss of fit caused by constraining
461 the observation model (e.g., via the ecological model) is an opportunity to measure the
462 discrepancy between observations and the assumed model and how much better/worse
463 the constrained model is than the null model, thus serving as a rational guide for model
464 improvement (Burnham & Anderson, 2010; Lunn et al., 2013).

465 We chose to conduct Bayesian posterior predictive checks for model evaluation and
466 model checking, because they are effective at identifying poorly fitted models without

467 requiring further data, although conservative when parameters are not estimated accu-
468 rately (Lunn et al., 2013). Other options (Conn et al. (2018) for a review) include cross-
469 validation, still possible in the case of models and data with a hierarchical structure, e.g.
470 using leave-one-out cross-validatory assessment or blocking, at a cost in terms of compu-
471 tational requirements (Marshall & Spiegelhalter, 2003; Roberts et al., 2017). We directly
472 compared catch (eq. (12)), although it would have been possible to compare the fit for
473 each size class using some measure involving both the data and the model, e.g., Pearson
474 χ^2 statistic, thus measuring the dissimilarity between the observed and modelled distribu-
475 tions in a manner close to a frequentist χ^2 test. The approach we used has the advantage
476 of telling about the direction of the poor fits (under- and over-estimates) while the χ^2
477 statistic allows to measure the fit at different scales (by summing the χ^2 statistics, e.g.,
478 over size classes to get a measure at the survey level). A χ^2 type statistic can also be used
479 to measure model fit for a wider range of models (Gelman et al., 2004; Ntzoufras, 2009;
480 Bal et al., 2014). We did not use the deviance statistic as a metric for model fit (Ntzoufras,
481 2009) either, due to the externalized computations it requires in the case of a model with
482 multiple error terms in the survey layer (in our case: Poisson and binomial). The scope
483 of our model checking was to evaluate the fitness of the survey layer given the estimated
484 length distribution. The model has five remaining random effects (see below), which were
485 consequently not subject to examination in our case, although this would still be possible
486 using replicated data and associated Bayesian p-values. The hierarchical framework offers
487 other options than the measure of absolute fit that can serve as a rational guide for model
488 improvement. We deem important mentioning the model comparison approach (Lunn
489 et al., 2013), either related to information theory such as the AIC (Burnham & Anderson,
490 2010), which seeks to identify which model would be the most efficient data compression
491 algorithm for the observed data, or fully Bayesian approaches (e.g., product space search;
492 see Tenan et al. (2014)), which seeks to identify which of the alternative models has the
493 highest relative credibility of being the true model, considering given data. In any case,
494 measuring the absolute fit as well as model selection benefits from an integrated approach,
495 by requiring formulation of the likelihood of model parameters given the data, which is a
496 direct result of expressing the observation process (‘external’ errors) in the model.

497 The HBM framework also allows for ‘internal’ errors or random effects, which account

498 for additional sources of variability. We did not use internal, additive errors for the
499 cohort mean sizes predicted by the growth model, as Lecomte & Laplanche (2012) did.
500 Our model thus represents an appreciable advance compared to theirs. We still considered
501 five random effects in the model, however: times of emergence ($d_{s,y}^{emerg}$), density of trout of
502 age 0+ ($\lambda_{s,y,1}$), apparent survival rate ($Sur_{s,y,k}$), growth rate (G'_s), and growth dispersion
503 rate (ν_s). All of these terms have an ecological meaning, the estimated values of which are
504 of great value by themselves. The drawback of having these random effects is that they
505 prevent using the model in its current state for inter- or extra-polation, either temporal
506 (e.g., forecasting) or spatial (e.g., to the stream continuum). All of these random effects,
507 however, open the possibility of adding a connection to covariates, since the framework
508 offers the ability to input spatio-temporal series of forcing variables into the model (e.g.,
509 water temperature).

510 We set parameters T^{min} , T^{opt} , and T^{max} as known and constant, using values from
511 laboratory experiments. The HBM framework makes it relatively easy to update the
512 model to adjust and estimate values of additional unknown parameters, since data are
513 informative, simply by defining these parameters as stochastic in the model (Ntzoufras,
514 2009; Lunn et al., 2013). The temperature range covered in our study area (0.7-23.2°C)
515 would make estimating these three parameters conceivable. We chose to use low informa-
516 tive priors for all of our parameters to facilitate a posteriori comparison of our estimates
517 to those of other studies. Another option is to tighten parameter priors by using results of
518 other studies (e.g., from Forseth et al. (2009) for T^{min} , T^{opt} , and T^{max}). In any case, the
519 flexibility offered by the HBM framework allows researchers to adjust and update their
520 model as a function of the knowledge available. It also allows modelling parameters as
521 functions of environmental covariates and random effects as residuals, using hyperparam-
522 eters that are considered to be perfectly known, partially known and defined with narrow
523 priors, or unknown and defined with vague priors.

524 4.2. Ecological results and discussion of main assumptions

525 We modelled the distribution of fish length as a mixture of Gaussian components,
526 which is the usual option (Pitcher, 2002). We have shown that the Gaussian mixture
527 model directly resulted from our growth model, which assumed that there are inter-

528 individual differences in growth rates and that fish individuals keep their advantages and
529 disadvantages over their life-time (Appendix A). Other studies have highlighted the im-
530 portance of inter-individual differences in growth traits and possible relative superiority or
531 inferiority among individual fish (Juanes et al., 2000; Peck et al., 2004; Biro et al., 2014).
532 We chose to model inter-individual differences in growth traits as random variation in
533 growth parameters, which is a standard approach (e.g., see Sainsbury (1980) or Tang
534 et al. (2014) with respect to the von Bertalanffy model). Our model led to a theoretical
535 relationship between the mean and standard deviation of the length distribution of each
536 cohort (i.e. proportional) that fitted our data well. Other authors have considered a con-
537 nection between the mean and standard deviation of length distributions, with CVs with
538 a range similar to ours (Lobón-Cervía & Rincón, 1998; Lobón-Cervía, 2010). The latter
539 authors, however, considered year-dependence, while we modelled site-dependence. Our
540 assumption of site-dependence could thus be relaxed into some spatio-temporal variation
541 ($\nu_{s,y}$), offering the ability to further study growth dispersion.

542 We modelled catchability as a logistic function of fish size and site (as in Ruiz &
543 Laplanche (2010)). The reasons for this choice included consideration of the increase in
544 catchability with increasing fish volume (Dolan & Miranda, 2003) as well as a dependence
545 on physical habitat. Some authors have considered other important covariates, such as
546 time (e.g., due to discharge), stream width (Letcher et al., 2015; Kanno et al., 2015), or
547 removal (Vøllestad et al., 2002; Laplanche, 2010). Although of little impact regarding
548 inference on growth, the relevance of the catchability model becomes crucial when inter-
549 preting estimates or when further modelling fish density (e.g., recruitment or mortality
550 rates).

551 We considered a Poisson model for fish dispersion, which seems acceptable in view
552 of the results of the posterior predictive checks, not issuing warnings with high numbers
553 of under- and over-estimates. The model assumes that the distribution of the fish of
554 a given size class in proximity of a sampled site is not spatially structured (Peterson,
555 1999). While riverine salmonid do not show gregarious behavior, due to strong intra-
556 specific competition, salmonid distribution can be patchy as a consequence of a spatial
557 structure of the physical habitat. In such cases, it would be necessary to consider another
558 statistical model for dispersion, e.g. using the negative binomial distribution, or expressing

559 dispersion as a function of physical habitat covariates.

560 We chose to model growth rate with a power function instead of the more widely used
561 von Bertalanffy growth function (He & Bence, 2007; Lecomte & Laplanche, 2012). Elliott
562 (2009) have suggested that salmonid growth is not asymptotic and that non-asymptotic
563 models should be used instead. Some studies have modelled *Salmo trutta* growth close
564 to linear (power growth model with $b = 0.31$; Elliott et al. (1995); Jensen (2003); Elliott
565 (2009); Forseth et al. (2009)), where we found a stronger curvature in this case study
566 ($b = 0.525$). To our point of view, however, EFRS data may not be the most appro-
567 priate tool for comparing growth models and to investigate whether salmonid growth
568 is asymptotic or not. The reason for this is that trout of age 2+ and older have rela-
569 tively low density and their length distributions overlap (Pitcher, 2002), thus providing
570 a low amount of information on trout growth. Information on individuals, either from
571 laboratory experiments or *in situ* via capture-recapture (Tang et al., 2014), seems more
572 appropriate. The choice of the empirical growth function becomes critical if estimating
573 the time of recruitment from length data becomes a priority, however. Age-dependence
574 of the growth rate due to gonad maturation and periodical changes in growth trajectories
575 could be approached with a biphasic growth model, still applicable in a HBM framework
576 (Quince et al., 2008; Dortel et al., 2013; Armstrong & Brooks, 2013; Higgins et al., 2015).
577 Finally, an alternative to empirical growth functions is to use a mechanistic, bioener-
578 getic model, such as Net Rate of Energy Intake (NREI) models, which simulate growth
579 of drift-feeding salmonids (Piccolo et al., 2014; Weber et al., 2014). NREI models are,
580 however, not applicable at large spatial scales due to their considerable data and com-
581 putationnal requirements (e.g., Hayes et al. (2007); Urabe et al. (2010)). Computational
582 requirements would also make such models impractical in a Bayesian framework, which
583 requires simulation of the ecological model at each iteration of the MCMC sampler.

584 We found that the density of trout of age 0+ varied greatly among sites and among
585 years, as usual with salmonids (Milner et al., 2003; Lobón-Cerviá, 2005; Vøllestad & Olsen,
586 2008). The number of trout of age 0+ present at survey times results from the combi-
587 nation of three ecological processes: spawning success the year before, survival between
588 spawning and emergence, and survival/movement (apparent survival) between emergence
589 and survey times. Survival between spawning and emergence may be related to environ-

590 mental conditions, due to high discharge damaging gravel redds before emergence (Kanno
591 et al., 2015). The same applies to apparent survival between emergence and survey times,
592 due to high discharge flushing parr following emergence, thus causing mortality and down-
593 stream movement (Jensen & Johnsen, 1999; Lobón-Cerviá, 2007; Nislow & Armstrong,
594 2012). Spatio-temporal variations in stream water temperature (via snowmelt) and in
595 precipitation (and resulting stream discharge) can thus cause large variations in the den-
596 sity of trout of age 0+ at survey times. Another reason is that adult spawning success
597 and competition of trout of age 0+ following emergence may be density-dependent (Mil-
598 ner et al., 2003; Liermann et al., 2010). Further variation in apparent survival strongly
599 depends on age and on season (Lobón-Cerviá & Rincón, 2004). Survival can decrease
600 significantly with increasing age in some rivers as a result of angling pressure, thus de-
601 creasing the apparent survival rate with increasing age, as we observed. Our population
602 dynamics model is basic in its current version and does not consider spawning success
603 nor stage-dependent survival rates. However, the HBM framework offers the possibility
604 to model population dynamics (Bret et al., 2017).

605 We found that a non-negligible portion of the growth rate was unrelated to water
606 temperature. Several studies have illustrated the ineffectiveness of water temperature
607 alone to predict salmonid growth rate in the wild (Table 1). A more recent meta-analysis
608 (Kovach et al., 2016) showed that temperature ‘was rarely related to growth’. On the
609 other hand, laboratory studies have reported a strong relationship between observed tem-
610 perature and growth (e.g., pseudo- $R^2 > 0.99$ in Elliott et al. (1995)). The latter study,
611 however, considered fish fed to satiation and consequently did not consider growth limi-
612 tation due to lack of food. The effect of temperature on growth is strongly mediated by
613 food consumption; the optimum temperature for growth varies considerably depending
614 on ration size (Brett et al., 1969; Elliott, 1975a,b; Piccolo et al., 2014). Since salmonids
615 are highly territorial and juvenile and subadult fish feed on benthic and drifting macro-
616 invertebrates (Oscoz et al., 2005; Johnson & McKenna, 2015; Johnson et al., 2017), *in*
617 *situ* food ration is likely related to intrinsic (conspecific density) and extrinsic factors
618 (discharge, macroinvertebrate density, etc.), which are the factors that were found to be
619 connected to salmonid growth (Table 1). Moreover, we found a strong connection between
620 growth rate and catchment area, which is considered as an integrated metric of habitat

621 capacity and incorporates habitat requirements at multiple scales (Rosenfeld, 2003; Lier-
622 mann et al., 2010; Ayllón et al., 2012). Our results thus corroborate those of other studies
623 indicating that growth rate is related to both water temperature and food ration, and
624 that this relationship remains predominant at a large spatial scale. We also conclude
625 that further modelling of the growth rate should include a relationship to environmental
626 variables related to daily food ration (e.g., discharge and macro-invertebrate density).

627 *4.3. Incorporating other kind of data/information*

628 Water temperature data are generally not available at EFRS sites, especially in the
629 case of long-term historical EFRS surveys initiated for management purposes. One pos-
630 sible consequence of using a model to predict water temperature is integrating finer scale
631 variation in water temperature and not detecting the resulting effect on growth, such as
632 thermally heterogeneous stream waters that fish exploit (Ruff et al., 2011; Armstrong
633 et al., 2013; Kanno et al., 2014). We predicted water temperature from air temperature
634 using a mixed-effects linear model, which is effective using monthly data (Caissie, 2006).
635 Making predictions at a finer temporal scale requires either a non-linear empirical model
636 (e.g., 4-parameter logistic, see Mohseni et al. (1998) or Bærum et al. (2013)) or a mecha-
637 nistic model, which requires more data (Caissie, 2006). We therefore kept a linear model,
638 in view of the large spatial (~ 10 -km between sites) and temporal (~ 1 year) sampling
639 frequency of our EFRS survey, which prevented us from evaluating the importance of
640 the effect of temperature on growth at a smaller spatiotemporal scale and removed the
641 need for water temperature values at a finer resolution. Moreover, our growth model
642 numerically integrates water temperature values (eq. (10)), which simulates the ecologi-
643 cal growth process in which fish integrate environmental conditions, thus decreasing the
644 effect of daily temperature variation on growth. Other studies have shown that modelling
645 water temperature as linear is a poor choice to capture a gradual shift in water temper-
646 ature (e.g., Bal et al. (2014)). We detected a spatial structure of the growth rate in the
647 downstream direction that we attributed to food availability rather than to temperature
648 increase, which was consistent with results of other studies (as discussed). Our thermal
649 model included the gradual shift in air temperature with elevation as well as a stream-
650 dependent thermal regime. For this reason, while we do not exclude the possibility that

651 our model missed a portion of the gradual shift in water temperature in the downstream
652 direction, it seems highly unlikely that the spatio-temporal variation of the growth rate
653 that we observed was due exclusively to water temperature. In any case, studying the ef-
654 fect of fine-scale thermal heterogeneity requires considering temperature data at a similar
655 scale (Ruff et al., 2011; Kanno et al., 2014).

656 We focused on juvenile and subadult stream-dwelling salmonids in upper streams, with
657 movements limited to switches between micro- and macro-habitat (Schlosser, 1991; Gido
658 & Jackson, 2010; White et al., 2014; Matthews & Hopkins, 2017; Laplanche et al., 2018).
659 This considerably reduces the impact of water temperature heterogeneity on growth.
660 While brown trout has high rates of site fidelity (Budy et al., 2008), other stream-dwelling
661 salmonids can move over larger distances (e.g., cutthroat trout, see Hilderbrand & Kersh-
662 ner (2000)). In such cases, a movement model should be considered, which would require
663 specific data such a fish’s successive locations using ITM (Hilderbrand & Kershner, 2000;
664 Marvin, 2012).

665 As indicated, salmonid growth may be predicted more accurately by modelling the
666 daily ration. Ration size depends mainly on fish size, macro-invertebrate drift density,
667 conspecific density, and discharge (Serchuk et al., 1980; Hughes & Grand, 2000; Weber
668 et al., 2014). Fish size and conspecific density are intrinsic model variables, which are
669 directly available in an integrated model. Discharge can be either directly measured *in*
670 *situ*, or predicted using hydrological models (e.g., the catchment-scale SWAT; Arnold et al.
671 (1998)). In the latter case, land use, soil type, topography and climate data including
672 precipitation are required as inputs, and measurement of discharge at the catchment outlet
673 is needed for discharge calibration. On the other hand, macro-invertebrate drift density
674 can be effectively sampled in rivers (Allan, 1987; Boyero et al., 2002; Hay et al., 2008).

675 Salmonid spawning is triggered mainly by photoperiod and temperature (Jonsson &
676 Jonsson, 2009) and is directly observable (timing and intensity) by monitoring spawning
677 grounds (Gallagher et al., 2007). The time required for development of trout eggs from
678 spawning to emergence is driven mainly by water temperature (Ojanguren & Braña, 2003;
679 Jonsson & Jonsson, 2009), which can be used to make accurate predictions of the time of
680 emergence (e.g., Elliott & Hurley (1998)). However, time of emergence is more difficult
681 to observe *in situ*, due to the small size of the emerged fry. Predictions and observations

682 of the times of spawning and emergence could be still incorporated into the model, in a
683 HBM framework (e.g., Lecomte & Laplanche (2012)).

684 We considered the parameters of the length-weight relationship as constant ($R^2 >$
685 0.99). Modelling seasonal growth variation, reproduction, or temporal variation in the
686 food ration might additionally require considering time-dependent length-weight param-
687 eters (Kimmerer et al., 2005; Froese, 2006). Moreover, studies in larger or more hetero-
688 geneous areas are expected to show larger spatial variation in length-weight parameters
689 (Froese, 2006). Spatial variation in length-weight parameters could be considered in this
690 case, even in a Bayesian framework (He et al., 2008), which would require additional
691 measurement of fish weight.

692 As stated, growth is strongly correlated with critical life history events. Development
693 of a growth model would serve the development of a population dynamics model by
694 providing access to growth-related variables (e.g., size, spawning time, emergence time).
695 As an illustration, mortality from angling could be modelled with an exponential decay
696 (see Serchuk et al. (1980); Lobón-Cerviá et al. (2012) for natural mortality), which would
697 be activated only during the angling season and to length classes which are above the
698 minimum legal capturable size.

699 *4.4. Conclusion*

700 Presentation of our model and results in their current form, and even more our sugges-
701 tions of model updates, both from growth and population dynamics perspectives, illustrate
702 that using a HBM allows for (1) modelling of ecological processes, (2) quantification of
703 measurement errors, and (3) links to covariates, resulting in (1) an increased range of eco-
704 logical applications, (2) improved hypothesis testing, and (3) increased predictive power,
705 which would allow researchers and managers to better understand a variety of salmonid
706 ecology issues at large spatio-temporal scales. Coupling our modelling approach to a
707 basin-scale hydrological model will expand the range of application of this HBM frame-
708 work, including the assessment of potential global change impacts on fish population
709 dynamics.

710 **Acknowledgements**

711 This study was undertaken under the research collaboration agreement between DEGN
 712 and Ecolab. Authors are grateful to all the DEGN staff involved in the collection and man-
 713 agement of electrofishing data since 1992, with special thanks to Javier Álvarez. Access to
 714 the HPC resources of CALMIP was granted under the allocation P1113. The authors ac-
 715 knowledge both anonymous reviewers for their insight and constructive comments which
 716 considerably improved the quality of this paper.

717 **Appendix A: Derivation of the growth model at the population level**

718 The growth of a fish individual is modelled as a consecutive length increase since its
 719 emergence

$$\frac{dL_i(t)}{dt} = H_{s,y}(t)(1 + \epsilon_i) \quad \text{for } t \geq d_i^{emerg}, L_i(d_i^{emerg}) = L_i^{emerg}$$

720 where i is an index on fish individuals, $L_i(t)$ is the length of individual i at time t ,
 721 $H_{s,y}(t)(1 + \epsilon_i)$ is its growth rate, L_i^{emerg} is its length at emergence that took place at time
 722 d_i^{emerg} . We assume that all the fish follow the same growth scheme, that is to say $H_{s,y}(t)$
 723 depends on the site s , on the year-of-emergence y , and on time t but not directly on i . On
 724 the other hand, we allow individuals to have superior/inferior growth rate with respect to
 725 each other and we assume that individuals keep their advantage ($\epsilon_i > 0$) or disadvantage
 726 ($\epsilon_i < 0$) over their life-time (similar to Sainsbury (1980) that used the von Bertalanffy
 727 model). We model variation in growth rate and size at emergence as independent and
 728 normally distributed variates, $\epsilon_i \sim \text{Normal}(0, \nu_s^2)$ and $L_i^{emerg} \sim \text{Normal}(L^{emerg}, \sigma^2)$. In
 729 this case, the length of individuals in a cohort at any time t is also normally distributed

$$L_i(t) \sim \text{Normal}(\mu_{s,y}(t), \sigma^2 + (\nu_s \Sigma H_{s,y}(t))^2),$$

730 by defining $\Sigma H_{s,y}(t) = \int_{d_{s,y}^{emerg}}^t H_{s,y}(u) du$ and $\mu_{s,y}(t) = L^{emerg} + \Sigma H_{s,y}(t)$. By assuming
 731 that variation due to variation in growth rate among individual fish overwhelms variation
 732 due to variation in emergence size and time ($\sigma^2 \ll (\nu_s \Sigma H_{s,y}(t))^2$), and in the case of
 733 juvenile and adult trout ($(L^{emerg})^2 \ll (\Sigma H_{s,y}(t))^2$), the length of individuals in a cohort
 734 is normally distributed as follows

$$L_i(t) \sim \text{Normal}(\mu_{s,y}(t), (\nu_s \mu_{s,y}(t))^2).$$

735 As a consequence, under such assumptions, fish length can be modelled as a mixture
736 of Gaussian distributions (eq. (6)), the mean size of each cohort ($\mu_{s,y}(t)$) is dictated by as
737 similar growth model (eq. (1)), and the standard deviation of the length of each cohort is
738 proportional to its mean (eq. (5)). The coefficient of variation (CV) is in the latter case
739 the standard deviation of the variate ϵ_i .

740 Supporting information

741 Additional Supporting Information may be found in the online version of this article.

- 742 • **Appendix S1.** Growth curves and temperature-dependence.
- 743 • **Appendix S2.** Model code and tutorial.
- 744 • **Appendix S3.** Water temperature.
- 745 • **Appendix S4.** Posterior distribution of top-level model parameters.

746 References

- 747 Ali, M., Nicieza, A., Wootton, R.J., 2003. Compensatory growth in fishes: a response to
748 growth depression. *Fish and Fisheries* 4, 147–190.
- 749 Allan, J.D., 1987. Macroinvertebrate drift in a Rocky Mountain stream. *Hydrobiologia*
750 144, 261–268.
- 751 Armstrong, D.P., Brooks, R.J., 2013. Application of hierarchical biphasic growth models
752 to long-term data for snapping turtles. *Ecological Modelling* 250, 119–125.
- 753 Armstrong, J.B., Schindler, D.E., Ruff, C.P., Brooks, G.T., Bentley, K.E., Torgersen,
754 C.E., 2013. Diel horizontal migration in streams: Juvenile fish exploit spatial hetero-
755 geneity in thermal and trophic resources. *Ecology* 94, 2066–2075.
- 756 Arnekleiv, J., Finstad, A., Ronning, L., 2006. Temporal and spatial variation in growth
757 of juvenile Atlantic salmon. *Journal of Fish Biology* 68, 1062–1076.

- 758 Arnold, J.G., Srinivasan, R., Muttiah, R.S., Williams, J.R., 1998. Large area hydrologic
759 modeling and assessment-Part 1: model development. *Journal of the American Water*
760 *Resources Association* 34, 73–89.
- 761 Ayllón, D., Almodóvar, A., Nicola, G.G., Parra, I., Elvira, B., 2012. Modelling carry-
762 ing capacity dynamics for the conservation and management of territorial salmonids.
763 *Fisheries Research* 134-136, 95–103.
- 764 Bærum, K.M., Haugen, T.O., Kiffney, P., Olsen, E.M., Vøllestad, L.A., 2013. Inter-
765 acting effects of temperature and density on individual growth performance in a wild
766 population of brown trout. *Freshwater Biology* 58, 1329–1339.
- 767 Bal, G., Rivot, E., Baglinière, J.L., White, J., Prévost, E., 2014. A hierarchical Bayesian
768 model to quantify uncertainty of stream water temperature forecasts. *PLoS ONE* 9.
- 769 Bal, G., Rivot, E., Prévost, E., Piou, C., Baglinière, J.L., 2011. Effect of water tempera-
770 ture and density of juvenile salmonids on growth of young-of-the-year Atlantic salmon
771 *Salmo salar*. *Journal of Fish Biology* 78, 1002–1022.
- 772 Banerjee, S., Carlin, B.P., Gelfand, A.E., 2004. Hierarchical modeling and analysis for
773 spatial data. Chapman and Hall/CRC.
- 774 Baumann, H., Talmage, S., Gobler, C., 2012. Reduced early life growth and survival in a
775 fish in direct response to increased carbon dioxide. *Nature Climate Change* 2, 38–41.
- 776 Bergerot, B., Hugueny, B., Belliard, J., 2015. Relating life-history traits, environmental
777 constraints and local extinctions in river fish. *Freshwater Biology* 60, 1279–1291.
- 778 Biro, P.A., Adriaenssens, B., Sampson, P., 2014. Individual and sex-specific differences in
779 intrinsic growth rate covary with consistent individual differences in behaviour. *Journal*
780 *of Animal Ecology* 83, 1186–1195.
- 781 Boithias, L., Acuña, V., Vergoñós, L., Ziv, G., Marcé, R., Sabater, S., 2014. Assessment
782 of the water supply: DEMand ratios in a Mediterranean basin under different global
783 change scenarios and mitigation alternatives. *Science of the Total Environment* 470-471,
784 567–577.

- 785 Boyero, L., Bosch, J., Nacional, M., Naturales, D.C., Abascal, J.G., 2002. Spatial and
786 temporal variation of macroinvertebrate drift in two neotropical streams 34, 567–574.
- 787 Bret, V., Capra, H., Gouraud, V., Lamouroux, N., Piffady, J., Tissot, L., Rivot, E., 2017.
788 Understanding inter-reach variation in brown trout (*Salmo trutta*) mortality rates using
789 a hierarchical Bayesian state-space model. Canadian Journal of Fisheries and Aquatic
790 Sciences 74, 1612–1627.
- 791 Brett, J., Shelbourn, J., Shoop, C., 1969. Growth rate and body composition of fingerling
792 sockeye salmon, *Oncorhynchus nerka*, in relation to temperature and ration size. Journal
793 of the Fisheries Research Board of Canada 26, 2363–2394.
- 794 Budy, P., Thiede, G.P., McHugh, P., Hansen, E.S., Wood, J., 2008. Exploring the relative
795 influence of biotic interactions and environmental conditions on the abundance and
796 distribution of exotic brown trout (*Salmo trutta*) in a high mountain stream. Ecology
797 of Freshwater Fish 17, 554–566.
- 798 Burnham, K., Anderson, D., 2010. Model selection and multimodel inference: a practical
799 information-theoretic approach. 2nd ed., Springer-Verlag.
- 800 Caissie, D., 2006. The thermal regime of rivers: a review. Freshwater Biology 51, 1389–
801 1406.
- 802 Chambert, T., Rotella, J.J., Higgs, M.D., 2014. Use of posterior predictive checks as
803 an inferential tool for investigating individual heterogeneity in animal population vital
804 rates. Ecology and Evolution 4, 1389–1397.
- 805 Clavero, M., Ninyerola, M., Hermoso, V., Filipe, A., Pla, M., Villero, D., Brotons, L.,
806 Delibes, M., 2017. Historical citizen science to understand and predict climate-driven
807 trout decline. Proceedings of the Royal Society of London B 284.
- 808 Coleman, M.A., Fausch, K.D., 2007a. Cold summer temperature limits recruitment of
809 age-0 cutthroat trout in high-elevation Colorado streams. Transactions of the American
810 Fisheries Society 136, 1231–1244.

811 Coleman, M.A., Fausch, K.D., 2007b. Cold summer temperature regimes cause a recruit-
812 ment bottleneck in age-0 Colorado River cutthroat trout reared in laboratory streams.
813 Transactions of the American Fisheries Society 136, 639–654.

814 Conn, P.B., Johnson, D.S., Williams, P.J., Melin, S.R., Hooten, M.B., 2018. A guide to
815 Bayesian model checking for ecologists. Ecological Monographs 0, 1–17.

816 Cowx, I.G., 1983. Review of the methods for estimating fish population size from survey
817 removal data. Aquaculture Research 14, 67–82.

818 Crozier, L.G., Zabel, R.W., Hockersmith, E.E., Achord, S., 2010. Interacting effects
819 of density and temperature on body size in multiple populations of Chinook salmon.
820 Journal of Animal Ecology 79, 342–349.

821 Dolan, C., Miranda, L., 2003. Immobilization thresholds of electrofishing relative to fish
822 size. Transactions of the American Fisheries Society 132, 969–976.

823 Dortel, E., Massiot-Granier, F., Rivot, E., Million, J., Hallier, J.P., Morize, E., Munaron,
824 J.M., Bousquet, N., Chassot, E., 2013. Accounting for Age Uncertainty in Growth
825 Modeling, the Case Study of Yellowfin Tuna (*Thunnus albacares*) of the Indian Ocean.
826 PLoS ONE 8, 1–12.

827 Elliott, J., 1975a. The growth rate of brown trout (*Salmo trutta* L.) fed on maximum
828 rations. Journal of Animal Ecology 44, 805–821.

829 Elliott, J., 1975b. The growth rate of brown trout (*Salmo trutta* L.) fed on reduced
830 rations. Journal of Animal Ecology 44, 823–842.

831 Elliott, J., Hurley, M., 1998. An individual-based model for predicting the emergence
832 period of sea trout fry in a Lake District stream. Journal of Fish Biology 53, 414–433.

833 Elliott, J., Hurley, M., Fryer, R., 1995. A new, improved growth model for brown trout,
834 *Salmo trutta*. Functional Ecology 9, 290–298.

835 Elliott, J.M., 2009. Validation and implications of a growth model for brown trout, *Salmo*
836 *trutta*, using long-term data from a small stream in north-west England. Freshwater
837 Biology 54, 2263–2275.

- 838 FAO Fisheries and Aquaculture Department, 2013. Fisheries and aquaculture software.
839 FISAT II - FAO-ICLARM Stock Assessment Tool. .
- 840 Filipe, A., Markovic, D., Pletterbauer, F., Tisseuil, C., De Wever, A., Schmutz, S.,
841 Bonada, N., Freyhof, J., 2013. Forecasting fish distribution along stream networks:
842 brown trout (*Salmo trutta*) in Europe. Diversity and Distributions 19, 1059–1071.
- 843 Forseth, T., Larsson, S., Jensen, A.J., Jonsson, B., Näslund, I., Berglund, I., 2009. Ther-
844 mal growth performance of juvenile brown trout \textit{Salmo trutta}: no support for
845 thermal adaptation hypotheses. Journal of Fish Biology 74, 133–149.
- 846 Froese, R., 2006. Cube law, condition factor and weight-length relationships: History,
847 meta-analysis and recommendations. Journal of Applied Ichthyology 22, 241–253.
- 848 Gallagher, S.P., Hahn, P.K.J., Johnson, D., 2007. Redd Counts, in: Johnson, D., Shrier,
849 B., O’Neil, J., Knutzen, J., Augerot, X., T.A., O., Pearson, T. (Eds.), Salmonid field
850 protocols handbook: techniques for assessing status and trends in salmon and trout
851 populations. American Fisheries Society, Bethesda, Maryland.
- 852 Gelman, A., Carlin, J.B., Stern, H.S., Rubin, D.B., 2004. Bayesian data analysis. Chap-
853 man and Hall/CRC.
- 854 Gido, K.B., Jackson, D.A., 2010. Community ecology of stream fishes: Synthesis and
855 future direction. American Fisheries Society Symposium 73, 651–664.
- 856 Grant, J.W.A., Imre, I., 2005. Patterns of density-dependent growth in juvenile stream-
857 dwelling salmonids. Journal of Fish Biology 67, 100–110.
- 858 Hay, C.H., Franti, T.G., Marx, D.B., Peters, E.J., Hesse, L.W., 2008. Macroinvertebrate
859 drift density in relation to abiotic factors in the Missouri River. Hydrobiologia 598,
860 175–189.
- 861 Hayes, J.W., Hughes, N.F., Kelly, L.H., 2007. Process-based modelling of inverte-
862 brate drift transport, net energy intake and reach carrying capacity for drift-feeding
863 salmonids. Ecological Modelling 207, 171–188.

- 864 He, J.X., Bence, J.R., 2007. Modeling annual growth variation using a hierarchical
865 Bayesian approach and the von Bertalanffy growth function, with application to lake
866 trout in southern Lake Huron. *Transactions of the American Fisheries Society* 136,
867 318–330.
- 868 He, J.X., Bence, J.R., Johnson, J.E., Clapp, D.F., Ebener, M.P., 2008. Modeling variation
869 in mass-length relations and condition indices of lake trout and Chinook salmon in
870 Lake Huron: a hierarchical Bayesian approach. *Transactions of the American Fisheries*
871 *Society* 137, 801–817.
- 872 Higgins, R.M., Diogo, H., Isidro, E.J., 2015. Modelling growth in fish with complex life
873 histories. *Reviews in Fish Biology and Fisheries* 25, 449–462.
- 874 Hilderbrand, R.H., Kershner, J.L., 2000. Movement patterns of stream-resident cutthroat
875 trout in Beaver Creek, IdahoUtah. *Transactions of the American Fisheries Society* 129,
876 1160–1170.
- 877 Hughes, N., Grand, T., 2000. Physiological ecology meets the ideal-free distribution: Pre-
878 dicting the distribution of size-structured fish populations across temperature gradients.
879 *Environmental Biology of Fishes* 59, 285–298.
- 880 Hutchings, J., 2002. Life histories of fish. Blackwell Science Ltd. volume 1 of *Handbook*
881 *of fish biology and fisheries*. pp. 149–174.
- 882 Imre, I., Grant, J.W., Cunjak, R.A., 2005. Density-dependent growth of young-of-the-year
883 Atlantic salmon *Salmo salar* in Catamaran Brook, New Brunswick. *Journal of Animal*
884 *Ecology* 74, 508–516.
- 885 Isely, J., Grabowski, T., 2007. Age and growth. American Fisheries Society, Bethesda.
886 Analysis and interpretation of freshwater fisheries data, pp. 184–228.
- 887 Jenkins, T., Diehl, S., Kratz, K., Cooper, S., 1999. Effects of population density on
888 individual growth of brown trout in streams. *Ecology* 80, 941–956.
- 889 Jensen, A., 2003. Atlantic salmon (*Salmo salar*) in the regulated River Alta: Effects

890 of altered water temperature on parr growth. *River Research and Applications* 19,
891 733–747.

892 Jensen, A., Forseth, T., Johnsen, B., 2000. Latitudinal variation in growth of young
893 brown trout *Salmo trutta*. *Journal of Animal Ecology* 69, 1010–1020.

894 Jensen, A., Johnsen, B., 1999. The functional relationship between peak spring floods
895 and survival and growth of juvenile Atlantic Salmon (*Salmo salar*) and Brown Trout
896 (*Salmo trutta*). *Functional Ecology* 13, 778–785.

897 Jobling, M., 2002. Life histories of fish. Blackwell Science Ltd. volume 1 of *Handbook of*
898 *fish biology and fisheries*. pp. 97–122.

899 Johnson, J.H., DiRado, J.A., Mackey, G., Abbett, R., 2017. Comparative diets and
900 foraging strategies of subyearling Atlantic salmon, brown trout, and rainbow trout
901 during winter. *Journal of Applied Ichthyology* 33, 1158–1165. doi:10.1111/jai.13488.

902 Johnson, J.H., McKenna, J.E., 2015. Diel Resource Partitioning among Juvenile Atlantic
903 Salmon, Brown Trout, and Rainbow Trout during Summer. *North American Journal*
904 *of Fisheries Management* 35, 586–597.

905 Jonsson, B., Jonsson, N., 2009. A review of the likely effects of climate change on anadro-
906 mous Atlantic salmon *Salmo salar* and brown trout *Salmo trutta*, with particular ref-
907 erence to water temperature and flow. *Journal of Fish Biology* 75, 2381–2447.

908 Juanes, F., Letcher, B.H., Gries, G., 2000. Ecology of stream fish: insights gained from
909 an individual-based approach to juvenile Atlantic salmon. *Ecology of Freshwater Fish*
910 9, 65–73.

911 Kanno, Y., Letcher, B., Hitt, N., Boughton, D.A., Wofford, J., Zipkin, E., 2015. Seasonal
912 weather patterns drive population vital rates and persistence in a stream fish. *Global*
913 *Change Biology* 21, 1856–1870.

914 Kanno, Y., Vokoun, J., Letcher, B., 2014. Paired stream-air temperature measurements
915 reveal fine-scale thermal heterogeneity within headwater brook trout stream networks.
916 *River research and applications* 30, 745–755.

- 917 Karpatne, A., Atluri, G., Faghmous, J.H., Steinbach, M., Banerjee, A., Ganguly, A.,
918 Shekhar, S., Samatova, N., Kumar, V., 2017. Theory-guided data science: A new
919 paradigm for scientific discovery from data. *IEEE Transactions on Knowledge and*
920 *Data Engineering* 29, 2318–2331.
- 921 Kaspersson, R., Höjesjö, J., 2009. Density-dependent growth rate in an age-structured
922 population: a field study on stream-dwelling brown trout *Salmo trutta*. *Journal of Fish*
923 *Biology* 74, 2196–2215.
- 924 Kéry, M., Schaub, M., 2012. Bayesian population analysis using WinBUGS: a hierarchical
925 perspective. Elsevier.
- 926 Kimmerer, W., Avent, S.R., Bollens, S.M., Feyrer, F., Grimaldo, L.F., Moyle, P.B.,
927 Nobriga, M., Visintainer, T., 2005. Variability in lengthweight relationships used to
928 estimate biomass of estuarine fish from survey data. *Transactions of the American*
929 *Fisheries Society* 134, 481–495.
- 930 Klemetsen, A., Amundsen, P.A., Dempson, J.B., Jonsson, B., Jonsson, N., O’Connell,
931 M.F., Mortensen, E., 2003. Atlantic salmon *Salmo salar* L., brown trout *Salmo trutta*
932 L. and Arctic charr *Salvelinus alpinus* (L.): a review of aspects of their life histories.
933 *Ecology of Freshwater Fish* 12, 1–59.
- 934 Kovach, R.P., Muhlfeld, C.C., Al-Chokhachy, R., Dunham, J.B., Letcher, B.H., Kershner,
935 J.L., 2016. Impacts of climatic variation on trout: a global synthesis and path forward.
936 *Reviews in Fish Biology and Fisheries* 26, 135–151.
- 937 Laplanche, C., 2010. A hierarchical model to estimate fish abundance in alpine streams by
938 using removal sampling data from multiple locations. *Biometrical Journal* 52, 209–221.
- 939 Laplanche, C., Elger, A., Thiede, G.P., Budy, P., 2018. Modeling the fish community
940 population dynamics and forecasting the eradication success of an exotic fish from an
941 alpine stream. *Biological Conservation* 223, 34–46.
- 942 Lecomte, J.B., Laplanche, C., 2012. A length-based hierarchical model of brown trout
943 (*Salmo trutta fario*) growth and production. *Biometrical Journal* 54, 108–126.

944 Letcher, B.H., Schueller, P., Bassar, R.D., Nislow, K.H., Coombs, J.A., Sakrejda, K.,
945 Morrissey, M., Sigourney, D.B., Whiteley, A.R., O'Donnell, M.J., Dubreuil, T.L., 2015.
946 Robust estimates of environmental effects on population vital rates: an integrated
947 capture-recapture model of seasonal brook trout growth, survival and movement in a
948 stream network. *Journal of Animal Ecology* 84, 337–352.

949 Levings, C.D., 2016. Ecology of salmonids in estuaries around the world: Adaptations,
950 habitats, and conservation. University of British Columbia Press.

951 Liermann, M.C., Sharma, R., Parken, C.K., 2010. Using accessible watershed size to pre-
952 dict management parameters for Chinook salmon, *Oncorhynchus tshawytscha*, popula-
953 tions with little or no spawner-recruit data: a Bayesian hierarchical modelling approach.
954 *Fisheries Management and Ecology* 17, 40–51.

955 Limpert, E., Stahel, W.a., Abbt, M., 2001. Log-normal Distributions across the Sciences:
956 Keys and Clues. *BioScience* 51, 341.

957 Lobón-Cerviá, J., 2005. Spatial and temporal variation in the influence of density de-
958 pendence on growth of stream-living brown trout (*Salmo trutta*). *Canadian Journal of*
959 *Fisheries and Aquatic Sciences* 62, 1231–1242.

960 Lobón-Cerviá, J., 2007. Numerical changes in stream-resident brown trout (*Salmo trutta*):
961 uncovering the roles of density-dependent and density-independent factors across space
962 and time. *Canadian Journal of Fisheries and Aquatic Sciences* 64, 1429–1447.

963 Lobón-Cerviá, J., 2010. Density dependence constrains mean growth rate while enhancing
964 individual size variation in stream salmonids. *Oecologia* 164, 109–115.

965 Lobón-Cerviá, J., Budy, P., Mortensen, E., 2012. Patterns of natural mortality in stream-
966 living brown trout (*Salmo trutta*). *Freshwater Biology* 57, 575–588.

967 Lobón-Cerviá, J., Rincón, P., 1998. Field assessment of the influence of temperature
968 on growth rate in a brown trout population. *Transactions of the American Fisheries*
969 *Society* 127, 718–728.

- 970 Lobón-Cerviá, J., Rincón, P.A., 2004. Environmental determinants of recruitment and
971 their influence on the population dynamics of stream-living brown trout *Salmo trutta*.
972 *Oikos* 105, 641–646.
- 973 Logez, M., Pont, D., 2011. Variation of brown trout *Salmo trutta* young-of-the-year growth
974 along environmental gradients in Europe. *Journal of Fish Biology* 78, 1269–1276.
- 975 Lunn, D., Jackson, C., Best, N., Thomas, A., Spiegelhalter, D., 2013. *The BUGS Book:*
976 *A practical introduction to Bayesian analysis*. Chapman and Hall/CRC.
- 977 Mallet, J., Charles, S., Persat, H., Auger, P., 1999. Growth modelling in accordance with
978 daily water temperature in European grayling (*Thymallus thymallus* L.). *Canadian*
979 *Journal of Fisheries and Aquatic Sciences* 56, 994–1000.
- 980 Marshall, E.C., Spiegelhalter, D.J., 2003. Approximate cross-validators predictive checks
981 in disease mapping models. *Statistics in Medicine* 22, 1649–1660.
- 982 Martins, E., Hinch, S., Cooke, S., Patterson, D., 2012. Climate effects on growth, phenol-
983 ogy, and survival of sockeye salmon (*Oncorhynchus nerka*): a synthesis of the current
984 state of knowledge and future research directions. *Reviews in Fish Biology and Fisheries*
985 22, 887–914.
- 986 Marvin, D., 2012. The Success of the Columbia Basin Passive Integrated Transponder
987 (PIT) Tag Information System, in: McKenzie, J. and Parsons, B. and Seitz, A. and
988 Kopf, R. and Mesa, M. and Phelps, Q. (Ed.), *Advances in Fish Tagging and Marking*
989 *Technology*, pp. 95–134.
- 990 Matthews, W.J., Hopkins, J., 2017. *Stream fish community dynamics: A critical synthesis*.
991 John Hopkins University Press, Baltimore.
- 992 Milner, N., Elliott, J., Armstrong, J., Gardiner, R., Welton, J., Ladle, M., 2003. The
993 natural control of salmon and trout populations in streams. *Fisheries Research* 62,
994 111–125.
- 995 Mohseni, O., Stefan, H., Erickson, T., 1998. A nonlinear regression model for weekly
996 stream temperatures. *Water Resources Research* 34, 2685–2692.

- 997 Myers, R.A., 2001. Stock and recruitment: Generalizations about maximum reproductive
998 rate, density dependence, and variability using meta-analytic approaches. *ICES Journal*
999 *of Marine Science* 58, 937–951.
- 1000 Myrvold, K.M., Kennedy, B.P., 2015. Density dependence and its impact on individual
1001 growth rates in an age-structured stream salmonid population. *Ecosphere* 6, 1–16.
- 1002 Naslund, I., Degerman, E., Nordwall, F., 1998. Brown trout (*Salmo trutta*) habitat use
1003 and life history in Swedish streams: possible effects of biotic interactions. *Canadian*
1004 *Journal of Fisheries and Aquatic Sciences* 55, 1034–1042.
- 1005 Nika, N., 2013. Change in allometric length-weight relationship of *Salmo trutta* at emer-
1006 gence from the redd. *Journal of Applied Ichthyology* 29, 294–296.
- 1007 Nislow, K.H., Armstrong, J.D., 2012. Towards a life-history-based management framework
1008 for the effects of flow on juvenile salmonids in streams and rivers. *Fisheries Management*
1009 *and Ecology* 19, 451–463.
- 1010 Ntzoufras, I., 2009. Bayesian modeling using WinBUGS. Wiley.
- 1011 Ojanguren, A., Braña, F., 2003. Thermal dependence of embryonic growth and develop-
1012 ment in brown trout. *Journal of Fish Biology* 62, 580–590.
- 1013 Oscoz, J., Leunda, P.M., Campos, F., Escala, M.C., Miranda, R., 2005. Diet of 0+ brown
1014 trout (*Salmo trutta* L., 1758) from the river Erro (Navarra, north of Spain). *Limnetica*
1015 24, 319–326.
- 1016 Parra, I., Almodóvar, A., Ayllón, D., Nicola, G.G., Elvira, B., 2011. Ontogenetic variation
1017 in density-dependent growth of brown trout through habitat competition. *Freshwater*
1018 *Biology* 56, 530–540.
- 1019 Parra, I., Almodóvar, A., Ayllón, D., Nicola, G.G., Elvira, B., 2012. Unravelling the
1020 effects of water temperature and density dependence on the spatial variation of brown
1021 trout (*Salmo trutta*) body size. *Canadian Journal of Fisheries and Aquatic Sciences* 69,
1022 821–832.

- 1023 Parra, I., Almodóvar, A., Nicola, G., Elvira, B., 2009. Latitudinal and altitudinal growth
1024 patterns of brown trout *Salmo trutta* at different spatial scales. *Journal of Fish Biology*
1025 74, 2355–2373.
- 1026 Peck, M.A., Buckley, L.J., Bengtson, D.A., 2004. Inter-individual differences in rates of
1027 routine energy loss and growth in young-of-the-year juvenile Atlantic cod. *Journal of*
1028 *Fish Biology* 64, 984–995.
- 1029 Pepin, P., 2016. Reconsidering the impossible - linking environmental drivers to growth,
1030 mortality, and recruitment of fish. *Canadian Journal of Fisheries and Aquatic Sciences*
1031 73, 205–215.
- 1032 Peterson, J.T., 1999. On the estimation of detection probabilities for sampling stream-
1033 dwelling fishes. Technical Report. BPA Report DOE/BP-25866-7. Bonneville Power
1034 Administration, Portland, Oregon.
- 1035 Piccolo, J.J., Frank, B.M., Hayes, J.W., 2014. Food and space revisited: The role of
1036 drift-feeding theory in predicting the distribution, growth, and abundance of stream
1037 salmonids. *Environmental Biology of Fishes* 97, 475–488.
- 1038 Pitcher, T., 2002. A bumpy old road: Sized-based methods in fisheries assessment. Black-
1039 well Science Ltd. volume 2 of *Handbook of fish biology and fisheries*. pp. 189–210.
- 1040 Quince, C., Abrams, P.A., Shuter, B.J., Lester, N.P., 2008. Biphase growth in fish I:
1041 Theoretical foundations. *Journal of Theoretical Biology* 254, 197–206.
- 1042 Quinn, T., 2005. The behavior and ecology of Pacific salmon and trout. Univ. WA Press,
1043 Seattle, WA, USA, 320 p.
- 1044 R Core Team, 2014. R: A Language and Environment for Statistical Computing. R
1045 Foundation for Statistical Computing. Vienna, Austria. .
- 1046 Riedl, C., Peter, A., 2013. Timing of brown trout spawning in Alpine rivers with special
1047 consideration of egg burial depth. *Ecology of Freshwater Fish* 22, 384–397.
- 1048 Rivot, E., Prévost, E., Cuzol, A., Baglinière, J.L., Parent, E., 2008. Hierarchical Bayesian
1049 modelling with habitat and time covariates for estimating riverine fish population size

1050 by successive removal method. *Canadian Journal of Fisheries and Aquatic Sciences* 65,
1051 117–133.

1052 Roberts, D.R., Bahn, V., Ciuti, S., Boyce, M.S., Elith, J., Guillera-Aroita, G., Hauen-
1053 stein, S., Lahoz-Monfort, J.J., Schröder, B., Thuiller, W., Warton, D.I., Wintle, B.A.,
1054 Hartig, F., Dormann, C.F., 2017. Cross-validation strategies for data with temporal,
1055 spatial, hierarchical, or phylogenetic structure. *Ecography* 40, 913–929.

1056 Robinson, J.M., Josephson, D.C., Weidel, B.C., Kraft, C.E., 2010. Influence of variable
1057 interannual summer water temperatures on brook trout growth, consumption, repro-
1058 duction, and mortality in an unstratified Adirondack lake. *Transactions of the American*
1059 *Fisheries Society* 139, 685–699.

1060 Rosenfeld, J., 2003. Assessing the habitat requirements of stream fishes: An overview and
1061 evaluation of different approaches. *Transactions of the American Fisheries Society* 132,
1062 953–968.

1063 Ruff, C.P., Schindler, D.E., Armstrong, J.B., Bentley, K.T., Brooks, G.T., Holtgrieve,
1064 G.W., McGlauffin, M.T., Torgersen, C.E., Seeb, J.E., 2011. Temperature-associated
1065 population diversity in salmon confers benefits to mobile consumers. *Ecology* 92, 2073–
1066 2084.

1067 Ruiz, P., Laplanche, C., 2010. A hierarchical model to estimate the abundance and
1068 biomass of salmonids by using removal sampling and biometric data from multiple
1069 locations. *Canadian Journal of Fisheries and Aquatic Sciences* 67, 2032–2044.

1070 Sainsbury, K., 1980. Effect of individual variability on the von Bertalanffy growth equa-
1071 tion. *Canadian Journal of Fisheries and Aquatic Sciences* 37, 241–247.

1072 Schlosser, I.J., 1991. Stream fish ecology: a landscape perspective. *BioScience* 41, 704–
1073 712.

1074 Serchuk, F., Schmitt, C., Floyd, B., 1980. Rainbow trout: a population simulation based
1075 on individual responses to varying environmental and demographic parameters. *Envi-*
1076 *ronmental Biology of Fishes* 5, 15–26.

- 1077 Sigourney, D.B., Munch, S.B., Letcher, B.H., 2012. Combining a Bayesian nonparametric
1078 method with a hierarchical framework to estimate individual and temporal variation in
1079 growth. *Ecological Modelling* 247, 125–134.
- 1080 Sogard, S.M., 1997. Size-Selective Mortality in the Juvenile Stage of Teleost Fishes: a
1081 Review. *Bulletin of Marine Science* 60, 1129–1157.
- 1082 Summerfeldt, R., Hall, G. (Eds.), 1987. Age and growth of fish. Iowa State University
1083 Press, Ames, Iowa. 544 pp.
- 1084 Tang, M., Jiao, Y., Jones, J.W., 2014. A hierarchical Bayesian approach for estimating
1085 freshwater mussel growth based on tag-recapture data. *Fisheries Research* 149, 24–32.
- 1086 Tenan, S., O’Hara, R.B., Hendriks, I., Tavecchia, G., 2014. Bayesian model selection:
1087 The steepest mountain to climb. *Ecological Modelling* 283, 62–69.
- 1088 Urabe, H., Nakajima, M., Torao, M., Aoyama, T., 2010. Evaluation of habitat quality
1089 for stream salmonids based on a bioenergetics model. *Transactions of the American*
1090 *Fisheries Society* 139, 1665–1676.
- 1091 Vøllestad, L., Olsen, E., Forseth, T., 2002. Growth-rate variation in brown trout in small
1092 neighbouring streams: evidence for density-dependence? *Journal of Fish Biology* 61,
1093 1513–1527.
- 1094 Vøllestad, L.A., Olsen, E.M., 2008. Non-additive effects of density-dependent and density-
1095 independent factors on brown trout vital rates. *Oikos* 117, 1752–1760.
- 1096 Weber, N., Bouwes, N., Jordan, C.E., 2014. Estimation of salmonid habitat growth poten-
1097 tial through measurements of invertebrate food abundance and temperature. *Canadian*
1098 *Journal of Fisheries and Aquatic Sciences* 71, 1158–1170.
- 1099 White, G.C., Burnham, K., 1999. Program MARK: survival estimation from populations
1100 of marked animals. *Bird Study* 46, 120–139.
- 1101 White, S.M., Giannico, G., Li, H., 2014. A ‘behaviorscape’ perspective on stream fish
1102 ecology and conservation: linking fish behavior to riverscapes. *Wiley Interdisciplinary*
1103 *Reviews: Water* 1, 385–400.

1104 Wyatt, R., 2002. Estimating riverine fish population size from single- and multiple-pass
1105 removal sampling using a hierarchical model. *Canadian Journal of Fisheries and Aquatic*
1106 *Sciences* 59, 695–706.

1107 Xu, C., Letcher, B.H., Nislow, K.H., 2010. Context-specific influence of water temperature
1108 on brook trout growth rates in the field. *Freshwater Biology* 55, 2253–2264.

Reference	Species	Age span	Data collection	Age determination	Data processing	Factor(s) affecting growth
Arnekleiv et al. (2006)	<i>S. salar</i>	0+, 1+, 2+	removal sampling	length	regression	discharge, temperature, density
Bal et al. (2011)	<i>S. salar</i> , <i>S. trutta</i>	0+	removal sampling	length	empirical model, HBM	density, temperature
Crozier et al. (2010)	<i>O. tshawytscha</i>	0+	removal sampling	length	regression	temperature, density
Grant & Imre (2005)	6 species	0+	removal sampling	length	regression	density
Jenkins et al. (1999)	<i>S. trutta</i>	0+	removal sampling	length	regression/ANOVA	density, location, year
Jensen et al. (2000)	<i>S. trutta</i>	0+, 1+, 2+, 3+	removal sampling	scale, otolith	empirical model	temperature
Kaspersson & Höjesjö (2009)	<i>S. trutta</i>	0+	tag	length, tag	regression/ANOVA	density, location
Letcher et al. (2015)	<i>S. fontinalis</i>	-	tag	length, tag	regression, HBM	temperature, discharge
Lobón-Cervía (2005)	<i>S. trutta</i>	0+, 1+, 2+, 3+	removal sampling	length, scale	regression/ANOVA	density, temperature
Parra et al. (2011)	<i>S. trutta</i>	0+, 1+, 2+	removal sampling	scale	regression	habitat availability
Parra et al. (2012)	<i>S. trutta</i>	0+, 1+, 2+	removal sampling	scale	quantile regression	density, temperature
Vøllestad & Olsen (2008)	<i>S. trutta</i>	0+	tag	length, scale, tag	regression/ANOVA	temperature, discharge, density
Xu et al. (2010)	<i>S. fontinalis</i>	0+, 1+, 2+, 3+, 4+	removal sampling, tag	length, tag	regression/ANOVA	temperature, discharge, density

Table 1: **Factor(s) affecting growth of stream-dwelling salmonids in the wild.** Studies using different salmonid species, age span, sampling method, proxy for age, and data processing method show the apparent wide variety of factors affecting salmonid growth in the wild.

Name	Description	Equation/value	Unit
Growth model			
b	power when weight grows linear	$\sim \text{Unif}(0, 1)$	1
ν_s	CV of cohort length	$\sim \text{Unif}(0, 1)$	1
$G_{s,y,k,d}$	growth rate	$= X_{s,y,d} G'_{s,y}$	% $\text{g}^b \cdot \text{day}^{-1}$
$\Sigma G_{s,y,k}$	cumulated growth rate	$= \sum_d G_{s,y,k,d}$	day
$X_{s,y,d}$	growth rate (deterministic effect)	=section 2.1.2	1
$G'_{s,y}$	growth rate (random effect)	$\sim \text{eq. (11)}$	% $\text{g}^b \cdot \text{day}^{-1}$
G'_s	growth rate (random effect; mean)	$\sim \text{Unif}(0, 10)$	% $\text{g}^b \cdot \text{day}^{-1}$
$\sigma_{G'_s}$	growth rate (random effect; s.d.)	$\sim \text{Unif}(0, 10)$	% $\text{g}^b \cdot \text{day}^{-1}$
T^{min}	minimum temperature for growth	$= 3.56$	$^{\circ}\text{C}$
T^{opt}	optimal temperature for growth	$= 13.11$	$^{\circ}\text{C}$
T^{max}	maximum temperature for growth	$= 19.48$	$^{\circ}\text{C}$
L^{emerg}	length at emergence	$= 30$	mm
$d_{s,y}^{emerg}$	median emergence time	$\sim \text{Unif}(\text{see text})$	day
a_w	weight/length scaling coefficient	$= 1.09 \cdot 10^{-5}$	g/mm^{b_w}
b_w	weight/length scaling exponent	$= 3.010$	1

Name	Description	Equation/value	Unit
Population dynamics model			
$\lambda_{s,y,1}$	density of trout of age 0+	$\sim \text{eq. (11)}$	trout.m $^{-2}$
λ_1	density of trout of age 0+ (mean)	$\sim \text{Unif}(0, 1)$	trout.m $^{-2}$
σ_{λ_1}	density of trout of age 0+ (s.d.)	$\sim \text{Unif}(0, 10)$	trout.m $^{-2}$
$\text{Sur}_{s,y,k}$	apparent survival rate	$\sim \text{eq. (11)}$	1
Sur_k	apparent survival rate (mean)	$\sim \text{Unif}(0, 1)$	1
$\sigma_{\text{Sur},k}$	apparent survival rate (s.d.)	$\sim \text{Unif}(0, 10)$	1
Observation model			
$d_{s,y}$	survey date	= known	day
x_{max}	max. trout length	400	mm
Δx	length class width	10	mm
$\mu_{s,y,k}$	mean of cohort length	= eq. (10)	mm
$\sigma_{s,y,k}$	s.d. of cohort length	$= \nu_s \mu_{s,y,k}$	mm
$\lambda_{s,y,k}$	density of 1+ and older ($k \geq 2$)	$= \text{Sur}_{s,y,k} \lambda_{y-1,s,k-1}$	trout.m $^{-2}$
$N_{s,y,l}$	population size	$\sim \text{eq. (7)}$	1
$C_{s,y,l,r}$	catch ('EFRS length data')	$\sim \text{eq. (8), data}$	1
$p_{s,y,l,r}$	catchability	$= \alpha_s x_l + \beta_s$	1
α_s	catchability parameter	$\sim \text{Unif}(-10, 10)$	m $^{-1}$
β_s	catchability parameter	$\sim \text{Unif}(-10, 10)$	1

Table 2: **Variables of the HBM.** Most variables are multi-dimensional, as indicated by their subscript (s, y, k, d, l, r ; Figure 2). Deterministic variables ($=$) are either measured without errors, known constant, or deterministic expressions from upper nodes. Stochastic variables (\sim) are either stochastic expressions from upper nodes or top-level random variables, in the latter case priors are indicated.

	Deterministic ($X_{s,d}$)	Random ($G'_{s,y}$)
site	10.3	73.0
year	1.5	2.5
month	30.6	–
site*year	1.2	24.5
site*month	24.7	–
site*day	31.7	–

Table 3: **Sources of variability of the daily growth rate.** Daily growth rate was modelled as the product of 3 terms: size-dependence, temperature-dependence ($X_{s,d}$), and other sources of variation ($G'_{s,y}$). The ANOVA sums of squares (SSQ; here in %) of $\log(X_{s,d})$ (using site, year, and month as factors; site*day refers to residuals) and $\log(G'_{s,y})$ (site and year; site*year refers to residuals) highlights the major sources of variability of these terms. Spatial variation of $G'_{s,y}$ is represented in Figure 7.

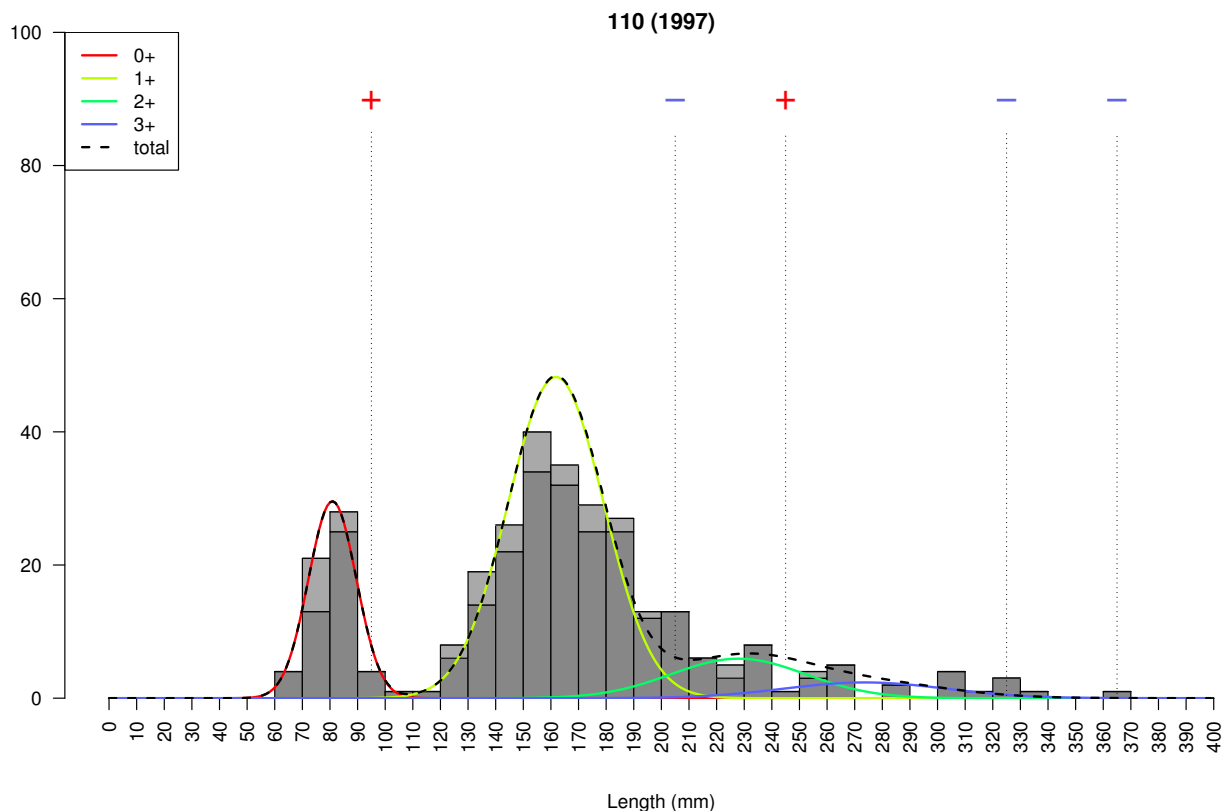


Figure 1: **Observations and model fit.** The histogram shows the number of fish caught (y-axis) in each length class (x-axis) for each removal (lower, dark grey stack: 1st removal; upper, light grey stack: 2nd removal). The distribution of fish length is modelled as a mixture of Gaussian components, one per age-class, which is here illustrated using point estimates of model parameters (red: trout of age 0+; yellow: 1+; green 2+; blue: 3+; black: sum). Fit is measured using posterior predictive checks, for each combination of site, year, and length class. A Bayesian p-value lower than 0.05 indicates an underestimated catch (minus signs in blue with vertical dotted lines) and a p-value greater than 0.95 indicates an overestimated catch (plus signs in red with vertical dotted lines). The survey conducted at site 110 in 1997 was here chosen as an example.

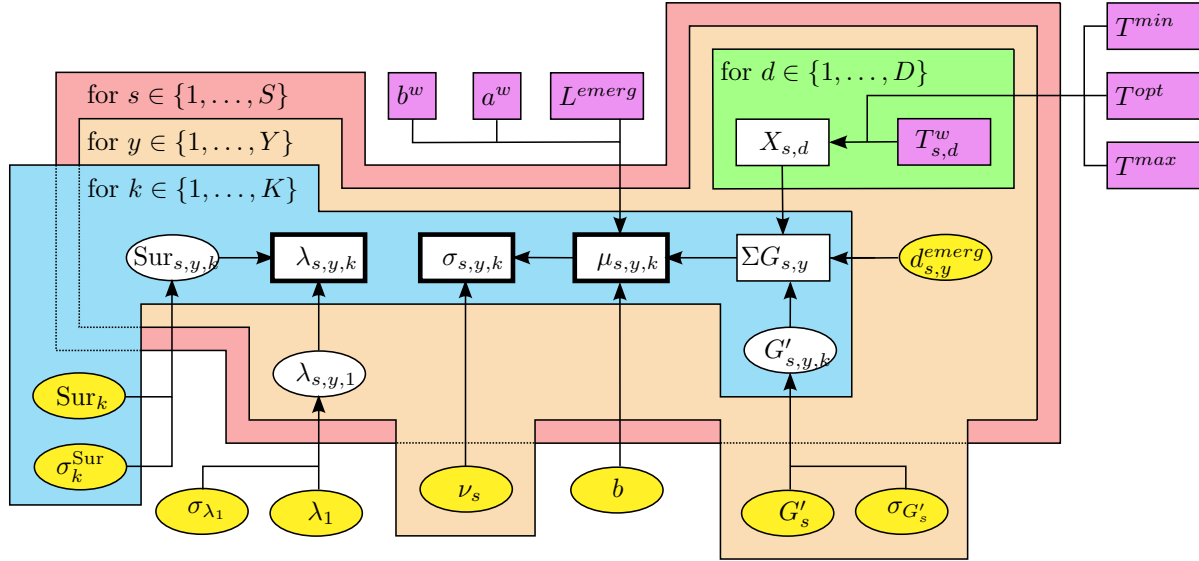


Figure 2: **Directed acyclic graph (DAG) of the growth and population dynamics components of the HBM.** Forcing variables and known parameters (in magenta) are connected to top-level parameters (yellow) via intermediate nodes (white). Variables are either deterministic (rectangles) or stochastic (ellipses) expressions. Variable equations/values are gathered together in Table 2. Most variables are multi-dimensional, as indicated by their subscripts and overlapping colour frames, one frame per index: site s (red); year-of-emergence y (orange); age k (blue); day d (green); variables outside frames are scalar. Brown trout length is modelled as a mixture of Gaussian distributions, which parameters (means $\mu_{s,y,k}$, standard deviations $\sigma_{s,y,k}$, and contributions $\lambda_{s,y,k}$ of each Gaussian component; rectangles with thick borders) are connected together with the growth and the population dynamics model (as represented) as well as to observations (not shown in this DAG, see text).

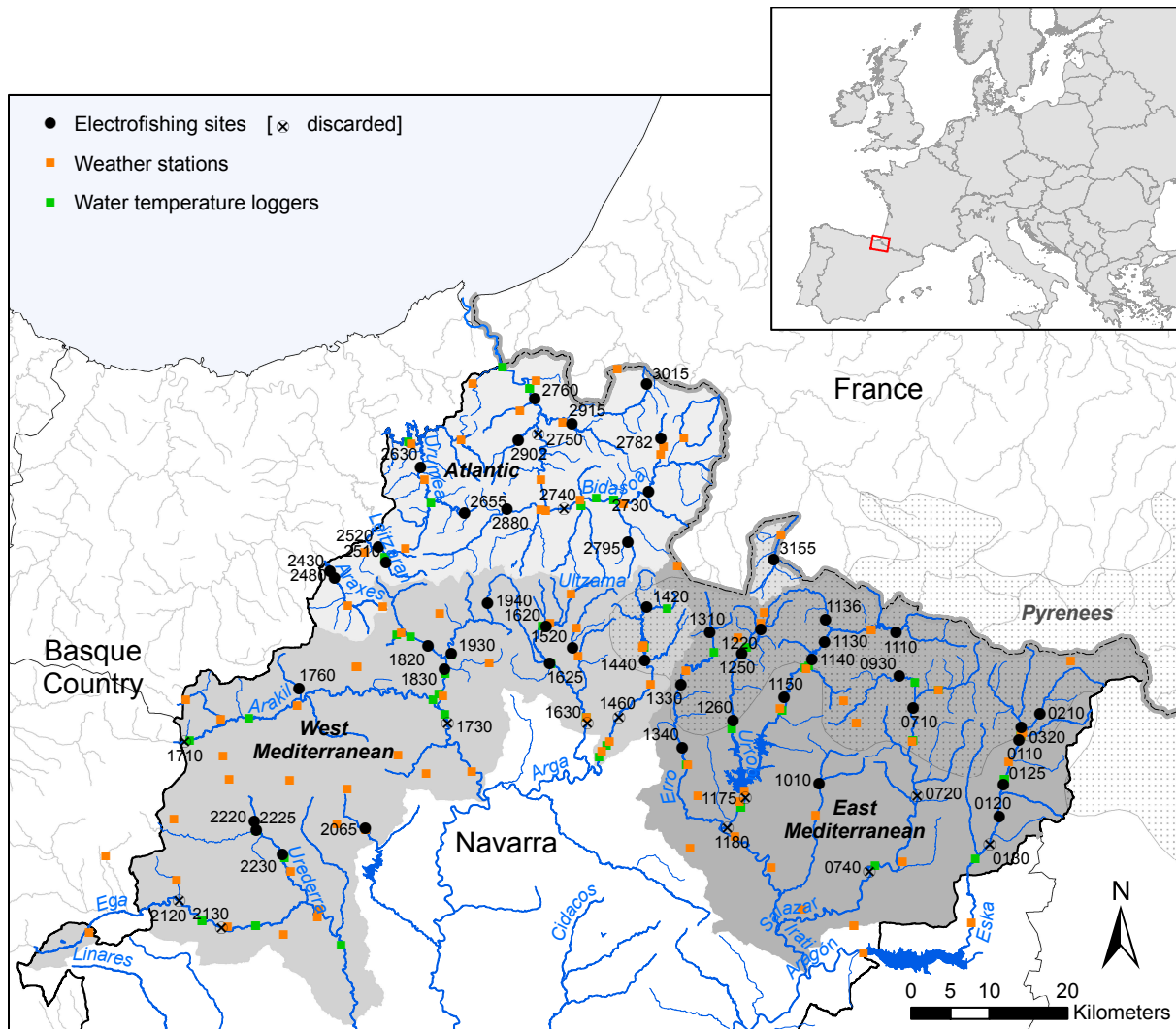


Figure 3: **Sampling design and study area.** The study area (6,420 km²) is the northern section of Navarra (thick black line: regional border) at the most western part of the Pyrenees mountain range (dotted area) in northern Spain (thick grey line: national border). The study area separates into 3 regions (grey areas): Atlantic to the Ega River; West Mediterranean to the Arga river; East Mediterranean to the Aragón river. A total of 61 sites (0110, ...) have been sampled by electrofishing once a year from 1992 to 2014. Only data from rivers unaffected by the presence of stocked individuals (48 sites; 1995–2014) were considered in the present analysis (black dots). Water (green dots) and air (orange) temperatures were also sampled in the area.

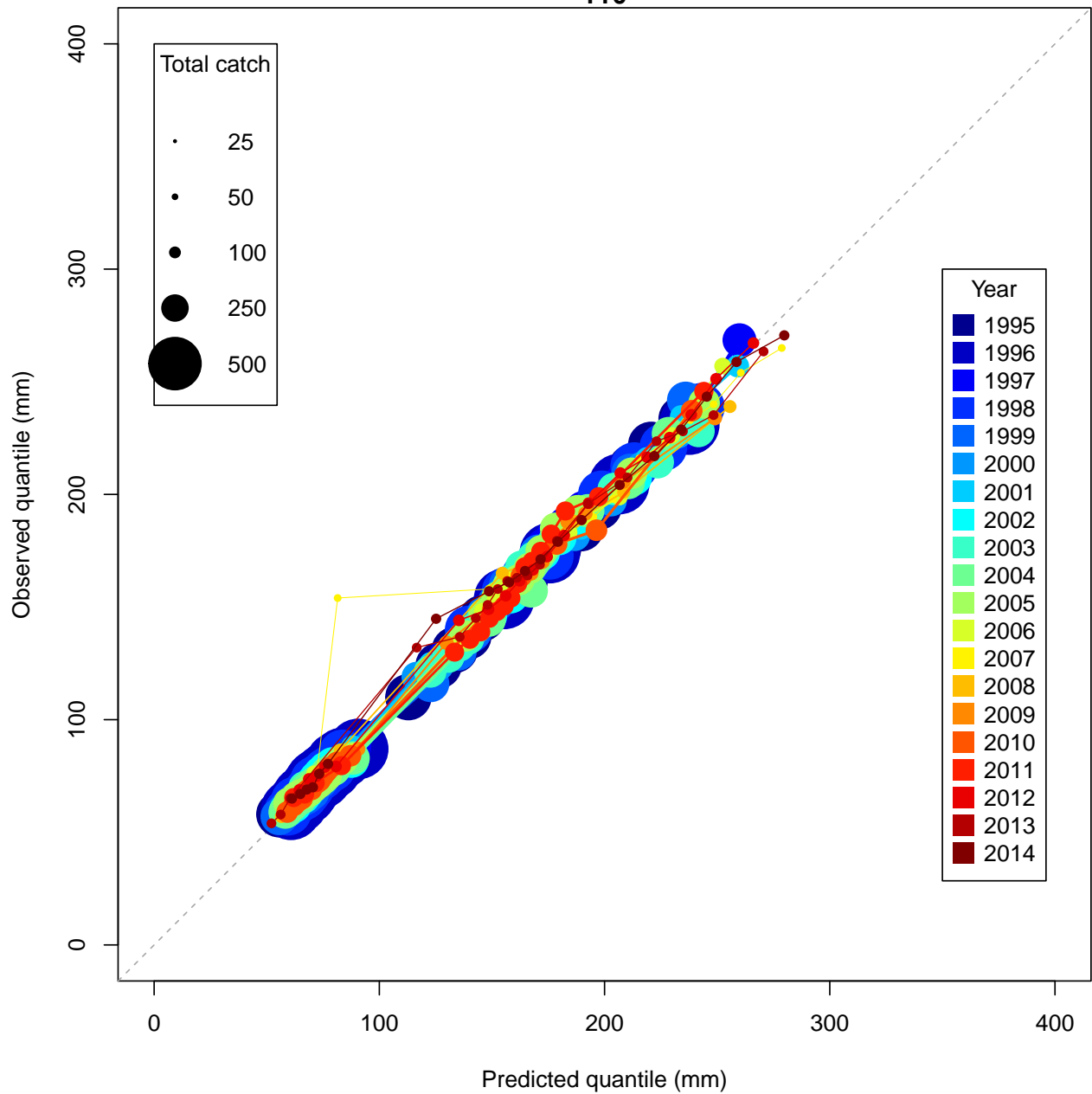


Figure 4: **QQ-plot of the predicted and observed distributions of fish length.** The quantiles of the predicted (x-axis) and observed (y-axis) multimodal distributions of fish length data (Figure 1) are plotted against each other for a graphical comparison of the two probability distributions. Quantiles were computed for probability values between 0.05 and 0.95 every 0.05 (one dot per probability interval), for each year (colour; see right legend), and for each site. Dot size (see left legend) is proportional to the total number of fish that were caught during surveys, thus highlighting scarce data. Site 110 was here chosen as an example.

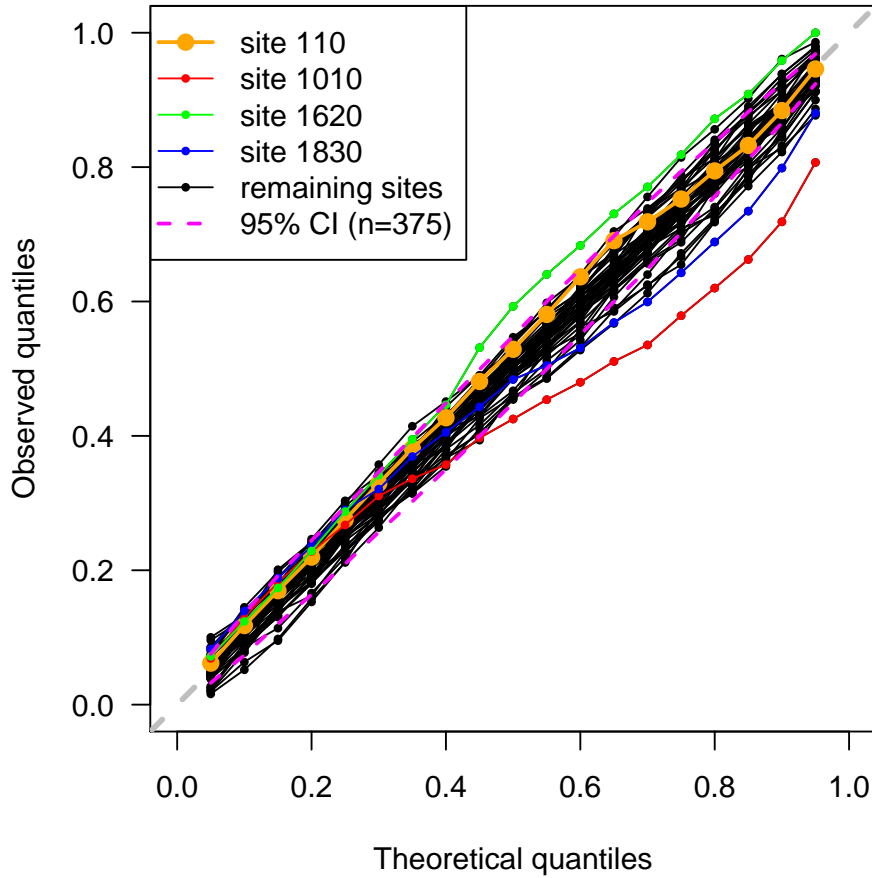


Figure 5: **QQ-plots of the Bayesian p-values of the posterior predictive checks.** The quantiles of the theoretical (x-axis) and observed (y-axis) distribution of the p-values of the posterior predictive checks are plotted against each other for a graphical comparison of the two probability distributions. P-values of the posterior predictive checks are uniformly distributed if the model fits correctly; the theoretical quantiles are thus those of the uniform (0,1) distribution. Quantiles were computed for probability values between 0.05 and 0.95 every 0.05 (one dot per probability interval), for each site (black lines; site 110 chosen as an example in Figures 1, 4, and 6 highlighted in orange). The number of p-values used to compute the QQ-plots ranges from 183 to 523 (375 ± 72.6), depending on the site. The model fits well, to the exception of site 1620 (green) with a larger number of significant overestimates (Bayesian p-values > 0.95), and sites 1010 (red) and 1830 (blue) due to extremely low fish density. The 95 % confidence interval on the estimates of the quantiles of a theoretically uniform (0,1) distribution using $n = 375$ samples is plotted (magenta) as an indication of the variation in the QQ-plots due to random sampling.

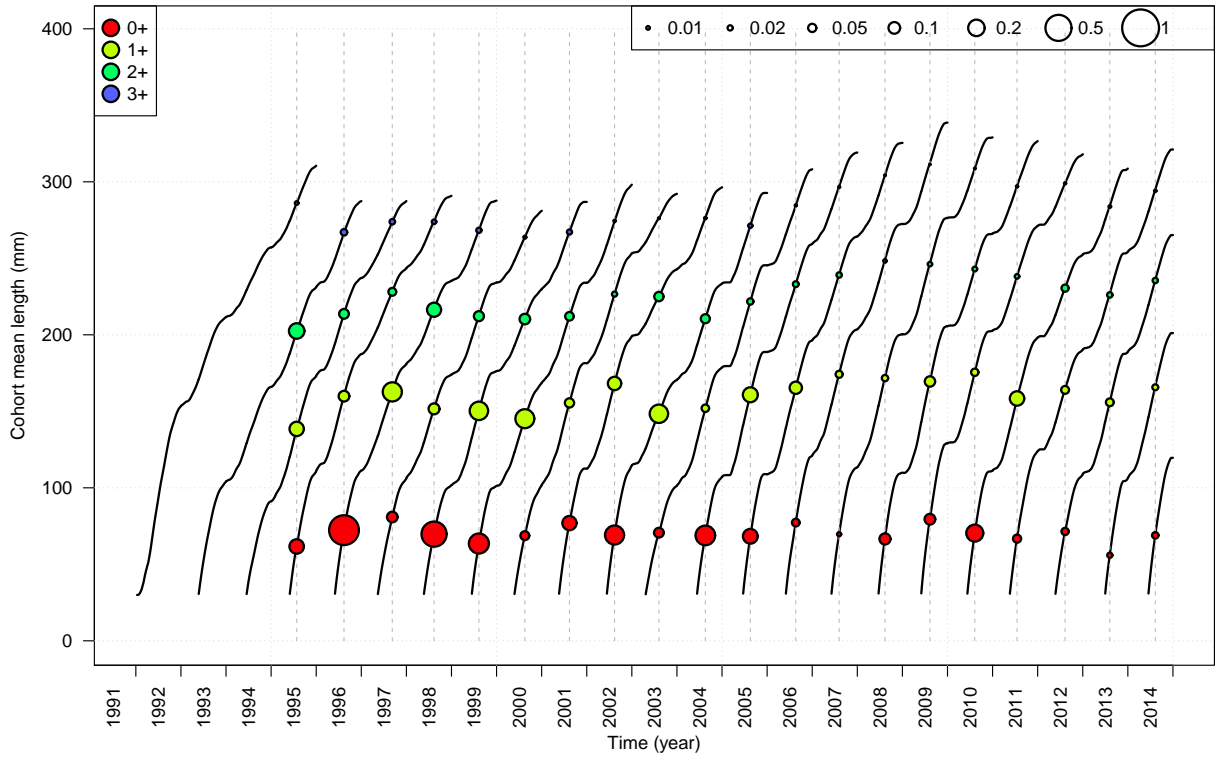


Figure 6: **Growth curves.** Growth of cohorts born in 1991–2014 was simulated at a daily time step at each site. Estimated values for growth parameters are used to compute the expected mean size of the cohorts at all times (so-called growth curves; black lines) starting from emergence. Temperature modulates growth which results in seasonal variation in fish size. Estimated densities at survey times are illustrated on the plot (circles, whose radius is proportional to density, see top-right legend; colour highlights trout age, see top-left legend; survey times are represented as vertical dashed grey lines). Mean sizes and densities are used to plot the modelled distribution of fish length at survey times (e.g., Figure 1 for 1997). Site 110 was chosen here as an example.

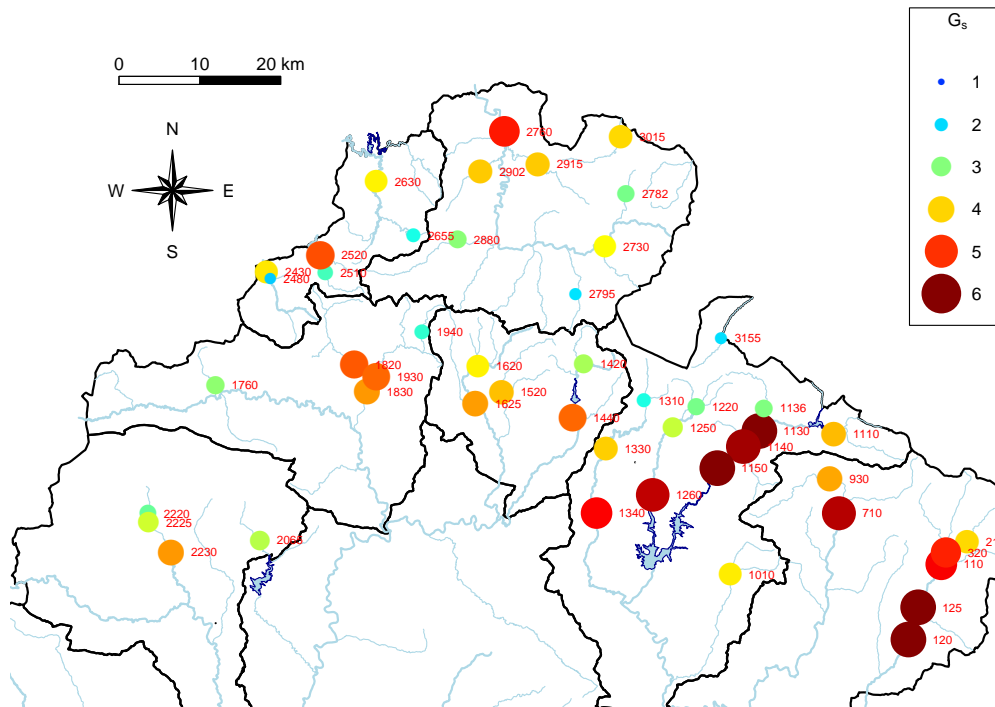


Figure 7: **Spatial variation in the growth rate.** Daily growth rate was modelled as the product of 3 terms: size-dependence, temperature-dependence, and other sources of variation ($G'_{s,y}$). The mean (denoted G'_s) at each site of $G'_{s,y}$ is represented on the map of the study area; G'_s increases in streams in the downstream direction. Results showed that G'_s is strongly correlated with catchment area ($r = 0.73$).